JNeurosci
THE JOURNAL OF NEUROSCIENCE

Research Articles: Development/Plasticity/Repair

Maintenance of Mouse Gustatory Terminal Field Organization is Dependent on BDNF at Adulthood

Chengsan Sun[1], Robin Krimm[2] and David L. Hill[1]

[1]*Department of Psychology, PO Box 400400, University of Virginia, Charlottesville, VA 22904-4400*
[2]*Robin F. Krimm, Department of Anatomical Sciences and Neurobiology, University of Louisville School of Medicine, Louisville, KY 40292*

DOI: 10.1523/JNEUROSCI.0802-18.2018

Received: 27 March 2018

Revised: 26 May 2018

Accepted: 17 June 2018

Published: 28 June 2018

Author contributions: C.S., R.F.K., and D.L.H. designed research; C.S., R.F.K., and D.L.H. performed research; C.S., R.F.K., and D.L.H. analyzed data; C.S., R.F.K., and D.L.H. edited the paper; D.L.H. wrote the first draft of the paper; D.L.H. wrote the paper.

Conflict of Interest: The authors declare no competing financial interests.

This work was supported by National Institutes of Health Grant DC000407 and DC006938 (to DLH) and DC007176 (to RFK). We thank Mr. Rolf Skyberg for comments on the manuscript.

Corresponding Author: Dr. David L. Hill, Department of Psychology, PO Box 400400, University of Virginia, Charlottesville, VA 22904, dh2t@virginia.edu, telephone: (434) 982-4728, fax: (434) 982-4785

Cite as: J. Neurosci ; 10.1523/JNEUROSCI.0802-18.2018

Maintenance of Mouse Gustatory Terminal Field Organization is Dependent on BDNF at Adulthood.

Chengsan Sun[1], Robin Krimm[2], and David L. Hill[1]
[1]Department of Psychology
PO Box 400400, University of Virginia,
Charlottesville, VA 22904-4400
and
[2]Robin F. Krimm
Department of Anatomical Sciences and Neurobiology
University of Louisville School of Medicine
Louisville, KY 40292

Abbreviated Title: BDNF Maintains Terminal Fields at Maturity

Corresponding Author: Dr. David L. Hill
Department of Psychology
PO Box 400400
University of Virginia
Charlottesville, VA 22904
dh2t@virginia.edu
telephone: (434) 982-4728
fax: (434) 982-4785

Number of pages: 44 pages

Number of figures: 5

Number of tables: 2

Number of words: Abstract – 249
Significance – 118
Introduction – 491
Discussion – 1500

Conflict of Interest: The authors declare no competing financial interests.

Acknowledgements: This work was supported by National Institutes of Health Grant DC000407 and DC006938 (to DLH) and DC007176 (to RFK). We thank Mr. Rolf Skyberg for comments on the manuscript.

ABSTRACT

The rodent peripheral gustatory system is especially plastic during early postnatal development and maintains significant anatomical plasticity into adulthood. Thus, taste information carried from the tongue to the brain is built and maintained on a background of anatomical circuits that have the capacity to change throughout the animal's lifespan. Recently, the neurotrophin, Brain Derived Neurotrophic Factor (BDNF), was shown to be required in the tongue to maintain normal levels of innervation in taste buds at adulthood, indicating that BDNF is a key molecule in the maintenance of nerve/target matching in taste buds. Here, we tested if maintenance of the central process of these gustatory nerves at adulthood also relies on BDNF by using male and female transgenic mice with inducible CreERT2 under the control of the Keratin 14 promoter or under control of the Ubiquitin promoter to remove *Bdnf* from the tongue or from all tissues, respectively. We found that the terminal fields of gustatory nerves in the nucleus of the solitary tract were expanded when *Bdnf* was removed from the tongue at adulthood, and with even larger and more widespread changes in mice where *Bdnf* was removed from all tissues. Removal of *Bdnf* did not affect numbers of ganglion cells that made up the nerves and did not affect peripheral, whole-nerve taste responses. We conclude that normal expression of *Bdnf* in gustatory structures is required to maintain normal levels of innervation at adulthood, and that the central effects of *Bdnf* removal are opposite of those in the tongue.

SIGNIFICANCE

BDNF plays a major role in the development and maintenance of proper innervation of taste buds. However, the importance of BDNF in maintaining innervation

patterns of gustatory nerves into central targets has not been assessed. Here, we tested if *Bdnf* removal from the tongue or from all structures in adult mice impacts the maintenance of how taste nerves project to the first central relay. Deletion of *Bdnf* from the tongue and from all tissues led to a progressively greater expansion of terminal fields. This demonstrates, for the first time, that BDNF is necessary for the normal maintenance of central gustatory circuits at adulthood and further highlights a level of plasticity not seen in other sensory system subcortical circuits.

INTRODUCTION

Impressive morphological, physiological, and behavioral changes characterize the postnatal development of the rodent gustatory system. This is especially evident for the age-related changes in neural circuits that transmit taste information from taste buds directly to the brain. The terminal field size of the nerves carrying taste information from taste buds directly to the nucleus of the solitary tract (NST) in the medulla decreases by as much as 4X within a 20 postnatal day period (Mangold and Hill, 2008; Zheng et al., 2014). This normal process can be interrupted by early embryonic and lifelong maternal dietary manipulations (May and Hill, 2006; Mangold and Hill, 2008) and by deleting the transduction channel for sodium salt taste throughout development (Sun et al., 2017). Surprisingly, these circuits remain plastic into adulthood. Sectioning two of three gustatory nerves at adulthood induces expansion of the intact nerve's terminal field by 5X within 15 days of the denervation (Corson and Hill, 2011). Moreover, inducibly deleting the sodium taste transduction channel at adulthood leads to an expanded organization similar to that found in immature animals (Skyberg et al., 2017). This

inherent and lifelong ability for taste neurons to remodel may be due, in part, to the continual turnover of taste bud cells throughout development. That is, the peripheral limb of these nerves must accommodate the change in receptive fields that occur approximately every 10 days (Beidler and Smallman, 1965).

Studies of nerve/target matching during development and maintenance of innervation in taste buds at adulthood point to the neurotrophin, Brain Derived Neurotrophic Factor (BDNF), as a likely candidate molecule regulating proper innervation by taste axons. BDNF regulates the initial innervation of taste buds by directing gustatory nerve fibers to their targets (Mbiene and Mistretta, 1997; Ma et al., 2009). It is then downregulated with age and expressed in a subpopulation of taste bud cells (Yee et al., 2003; Huang and Krimm, 2010). Although emerging evidence supports BDNF as being critical during development of peripheral gustatory circuits, the extent it is required for maintenance of these circuits at adulthood is unclear. Recently, Meng et al. (2015) did the first study to examine the effects of BDNF removal at adulthood on the maintenance of innervation patterns in the gustatory system. They genetically removed BDNF from taste bud cells in adult mice, and showed a 40% loss of taste bud innervation and some taste bud cells. Maintenance of the peripheral innervation pattern was not retained.

If BDNF is required to maintain the innervation of taste buds at adulthood, we asked here if it is also required to maintain the central limb of these same nerves. We used the same genetic strategy as Meng et al. (2015) to inducibly delete *Bdnf* from taste bud cells or from all tissues, and found that the terminal field sizes dramatically increased

in the brainstem. Thus, the same experimental manipulation led to opposite effects on the central process of gustatory nerves compared to that on the peripheral process.

MATERIALS AND METHODS

Animals. All experiments were approved by the University of Virginia Animal Care and Use Committee and followed guidelines set forth by the National Institutes of Health and the Society for Neurosciences. Experimental animals were transgenic mice in which the gene for *Bdnf* was inducibly removed from the tongue or from all cells at adulthood. These animals were made, respectively, by crossing mice that expressed CreERT2 under control of the Keratin 14 promoter (https://www.jax.org/strain/005107: RRID:IMSR_JAX:005107) or under control of the Ubiquitin promoter (https://www.jax.org/strain/007001: RRID:IMSR_JAX:007001) with mice in which exon 5 of the *Bdnf* gene was floxed (https://www.jax.org/strain/004339: RRID:IMSR_JAX:004339). We, and others (Meng et al., 2015), found that 60-80% of *Bdnf* expression in the tongue remained in both groups of mice following a single injection of 6 mg tamoxifen, as measured by real-time transcription-polymerase chain reaction (qPCR). To decrease the amount of *Bdnf* expression to much lower levels, we bred mice so that one of the alleles was null for *Bdnf* (https://www.jax.org/strain/002266: RRID:IMSR_JAX:002266) and the other allele was floxed. We also increased the administration of tamoxifen (T5648, Sigma, St. Louis, MO; mixed in corn oil, 188 ng/g body weight) to once each weekday for 3 weeks. Tamoxifen was delivered by oral gavage (Ruzankina et al., 2007), beginning at 40 days of age. No treatment was administered during the weekends. Therefore, our experimental animals had the genotype of K14-CreER $Bdnf^{flox/-}$TAM or UBC-CreER $Bdnf^{flox/-}$TAM for mice in which *Bdnf*

130 expression was deleted from the tongue or from all cells, respectively. For clarity, we will
131 refer to these two inducible knockout mice as K14-*Bdnf* iKO and UBC-*Bdnf* iKO mice,
132 respectively.

133 Two control groups were used for comparisons with the two experimental groups.
134 One group consisted of mice that were littermates to experimental animals, but did not
135 have any of the transgenes (Control; $Bdnf^{+/+}$). Another group had all of the transgenes for
136 K14-CreER $Bdnf^{lox/-}$ mice or for UBC-CreER $Bdnf^{lox/-}$ mice, but did not receive
137 administration of tamoxifen (K14-*Bdnf* iKO No TAM and UBC-*Bdnf* iKO No TAM,
138 respectively). Thus, these latter two groups were used to control for the effects of the
139 heterozygous removal of the *Bdnf* gene throughout development.

140 *Tissue Collection*. To establish that mice used here had reduced *Bdnf* expression in the
141 anterior tongue, geniculate ganglion, and in the nucleus of the solitary tract (NST), we
142 used qPCR procedures similar to that described by Huang and Krimm (2010) and Sun et
143 al. (2015). Briefly, the anterior 2/3 of fresh tongues from mice (Controls, n=3: 2 males, 1
144 female; K14-*Bdnf* iKO No TAM; n=6: 3 males, 3 females; K14-*Bdnf* iKO; n=7: 3 males,
145 4 females; UBC-*Bdnf* iKO No TAM; n=6: 3 males, 3 females; UBC-*Bdnf* iKO; n=6: 4
146 males, 2 females) were collected and cut at the midline, rinsed with cold PBS, and then
147 incubated in sterile dispase I-solution (BD Biosciences; San Jose, CA) for 60 min at
148 37°C. Epithelial sheets of the tongue were then peeled from the underlying mesenchyme
149 and transferred into separate tubes containing RNAlater (ThermoFisher Scientific,
150 Waltham, MA), and then stored at −80°C until RNA extraction. Epithelial sheets of the
151 tongue were then peeled from the underlying connective tissue for RNA extraction.
152 Similarly, fresh geniculate ganglia (Controls, n=3: 2 males, 1 female; K14-*Bdnf* iKO No

153 TAM; n=3: 1 male, 2 females; K14-*Bdnf* iKO; n=7: 3 males, 4 females; UBC-*Bdnf* iKO
154 No TAM; n=3: 2 males, 1 female; UBC-*Bdnf* iKO; n=3: 2 males, 1 females) and the
155 rostral portion of the NST (Controls, n=5: 2 males, 3 females; K14-*Bdnf* iKO No TAM;
156 n=5: 2 males, 3 females; K14-*Bdnf* iKO; n=5: 2 males, 3 females; UBC-*Bdnf* iKO No
157 TAM; n=5: 3 males, 2 females; UBC-*Bdnf* iKO; n=3: 2 males, 1 female) were dissected
158 and transferred into separate tubes containing RNAlater (Ambion, Austin, TX), and then
159 stored at −80°C until RNA extraction. Fresh geniculate ganglia were collected after
160 removal of the brain and visualized within the ventral cranium. The rostral NST was
161 removed after horizontally sectioning the brainstem with a vibratome at 200 μm in cold
162 PBS. The region of interest (anterior half of the NST) was removed with a sterile scalpel
163 under a dissecting microscope. The NST is visible in unstained tissue and can be easily
164 seen as a clear structure compared to surrounding tissue. Brainstem landmarks (e.g., 4th
165 ventricle, solitary tract, hypoglossal nucleus) were used to identify dorsal to ventral
166 extents of the NST.
167 *RNA Extraction and Measurement*. Total RNA from anterior tongue epithelia, geniculate
168 ganglia, and NST, was extracted as described previously (Huang and Krimm, 2010; Sun
169 et al., 2015). RNA Integrity Numbers (RIN) were used to estimate the RNA quality. Only
170 RNA samples with RIN more than 8.0 were used. The same amount of RNA from control
171 and tamoxifen-treated mice was used. RNA was also treated in parallel in the absence of
172 reverse transcriptase to examine for genomic DNA contamination. qPCR was performed
173 by 7500 Fast Real-Time PCR System (Applied Biosystems, Foster City, CA), using
174 TaqMan Universal PCR kit (Applied Biosystems, Foster City, CA) and oligonucleotide
175 primer/probe sets (Huang and Krimm, 2010; Sun et al., 2015). TaqMan probes were

labeled at the 5′-end with a fluorescent reporter dye (FAM) and at the 3′-end with a quencher dye (TAMRA).

The sequences of primers and probes are as following:

BDNF (Forward primer, TGCAGGGGCATAGACAAAAGG;

Reverse primer, CTTATGAATCGCCAGCCAATTCTC;

Probe, ACTGGAACTCGCAATGCCGAACTACCCA),

GADPH (Forward primer, CTGGGACGACATGGAGAAGATC;

Reverse primer, CAACCTGGTCCTCAGTGTAGC;

Probe, CGTGCCGCCTGGAGAAACCTGCC).

qPCR reactions were performed in a 20μl total volume with 1 × Master Mix, 720/200 nM primer/probe sets. PCR efficiencies were determined by performing PCR with serial (10-fold) dilutions of cDNA in parallel. All samples were run in parallel with the housekeeping gene, mouse glyceraldehyde 3-phosphate dehydrogenase (GAPDH), to normalize cDNA loading. Each assay was carried out in triplicate. PCR was performed for 40 cycles at 95°C for 15 secs and at 60°C for 1 min.

qPCR Analyses. For qPCR, the comparative $2^{-\Delta\Delta CT}$ method was used to determine the relative *Bdnf* gene expression levels (Huang and Krimm, 2010; Sun et al., 2015). The normalized expression of the *Bdnf* was calculated as normalized expression = $(E_{BDNF})^{\Delta CT}{}_{target(control\ -\ sample)}/\ (E_{ref})^{\Delta CT}{}_{GAPDH(control\ -\ sample)}$. E_{Bdnf} and E_{GAPDH} represent the reaction efficiency of the respective gene, and ΔCT is the cycle difference between the control and the sample.

BDNF Immunohistochemistry. To examine if the group-related effects of *Bdnf* expression are reflected in the presence of BDNF in the NST, we did immunohistochemical

experiments that focused on the NST in UBC-*Bdnf* iKO mice. Two control (1 male and 1 female) and two UBC-*Bdnf* iKO mice (1 male and 1 female) were perfused as described in nerve labeling section. Sections were then incubated in BDNF antibody raised in rabbit at a concentration of 1:200 (Alomone Labs; ANT-010; RRID:AB_2039756) in 1% BSA and 0.3% Triton X-100 in 0.1 M PBS overnight. After rinsing with PBS (6 X 10 min), sections were incubated in a Donkey anti-rabbit secondary antibody conjugated with 1:400 AlexaFluor-488 (Jackson ImmunoResearch Labs, Inc.; 711-545-152; RRID:AB_2313584) for 1.5 hours. Then sections were rinsed and mounted on slides and examined on a fluorescent microscope at 10X and 20X.

Fluorescent Anterograde Nerve Labeling. Procedures used to fluorescently label the chorda tympani (CT), which innervates taste buds on the anterior two-thirds of the tongue, the greater superficial petrosal nerve (GSP), which innervates taste buds on the palate, and the glossopharyngeal nerve (IX), which innervates taste buds on the posterior tongue, were the same as that described previously in mouse (Sun et al., 2015; Sun et al., 2017). Briefly, the CT, GSP, and IX nerves were labeled in 6 (3 males; 3 females) controls, 3 (1 male; 2 females) K14-*Bdnf* iKO No TAM, 7 (3 males; 4 females) K14-*Bdnf* iKO, 4 (2 males; 2 females) UBC-*Bdnf* iKO No TAM, and 5 (3 males; 2 females) UBC-*Bdnf* iKO mice with anterograde tracers to determine the volume and densities of label among gustatory afferent terminal fields in the NST. All animals were between 4 and 5 months old at the time of nerve labeling. Therefore, for experimental groups, the nerve labeling occurred approximately 60 days following the last administration of tamoxifen. The anterograde labeling surgery for mice in the two control groups were aged-matched with the experimental groups. Mice were sedated with a 0.32 mg/kg injection of

Domitor® (medetomidine hydrochloride: Pfizer Animal Health, Exton, PA; I.M.) and anesthetized with 40 mg/kg Ketaset® (ketamine hydrochloride: Fort Dodge Animal Health, Fort Dodge, IA; I.M.). A water-circulating heating pad was used to maintain body temperature. Using the same surgical approach as detailed in Sun et al. (2015; 2017), the CT and GSP nerves were cut near and peripheral to the geniculate ganglion in the tympanic bulla and crystals of 3kD tetramethylrhodamine dextran amine were then applied to the proximal cut end of the GSP, and 3kD biotinylated dextran amine was applied to the proximal cut end of the CT. A small amount of Kwik-Sil (World Precision Instruments, Inc.; Sarasota, FL) was then placed over the cut end of the nerves to prevent crystals from diffusing from the site of the intended label. The IX was isolated medial to the tympanic bulla and was cut peripheral to the petrosal ganglion and placed on a small piece of parafilm. Crystals of 3kD cascade blue dextran amine were applied to the proximal cut end of the IX nerve. All dextran amine conjugates were purchased from Life Technologies (Grand Island, NY). Vaseline and a layer of parafilm were placed on top of the IX to keep the dextran in place. Animals were then injected with 5 mg/ml Antisedan® (atipamezole hydrochloride: Pfizer Animal Health, Exton, PA; I.M) to promote reversal of anesthesia. Following 48-hour survival, animals were deeply anesthetized with urethane and transcardially perfused with Krebs-Henseleit buffer (pH 7.3), followed by 4% paraformaldehyde (pH 7.2).

Tissue preparation. Brains were removed, postfixed, and the medulla was blocked and sectioned horizontally on a vibratome at 50µm (Sun et al., 2015; Sun et al., 2017). We sectioned tissue in the horizontal plane because it allows visualization of the entire rostral-caudal and medial lateral extent of the terminal fields in the NST with the smallest

number of sections (~10 sections/mouse), and is also the plane in which the axons branch from the solitary tract and project primarily medially in rodents (Davis, 1988; Whitehead, 1988; Lasiter et al., 1989). Highly-detailed descriptions of the mouse NST and the projection of the CT to this nucleus and subnuclei have been described in coronal sections (Bartel and Finger, 2013; Ganchrow et al., 2014). Therefore, we also sectioned brainstems in coronal section to qualitatively examine group-related differences in the innervation of NST subnuclei.

Sections were incubated for 1 hour in PBS containing 0.2% Triton with 1:500 streptavidin Alexa Fluor 647 (Jackson ImmunoResearch Labs, Inc., West Grove, PA; 016-600-084; RRID: AB_2341101) and 1:500 rabbit anti-Cascade Blue (ThermoFisher Scientific, Waltham, MA; A-5760; RRID: AB_2536192) at room temperature. Streptavidin Alexa Fluor 647 was used to visualize the biotinylated dextran amine-labeled CT positive terminals. Rabbit anti-Cascade Blue was used as a primary antibody to detect Cascade Blue labeled IX terminal fields and was followed with a 1 hr. reaction with 1:500 goat anti-rabbit Alexa Fluor 488 (ThermoFisher Scientific, Waltham, MA; A-21206, RRID: AB_2535792). This secondary antibody was used to visualize IX nerve terminals. Visualization of tetramethylrhodamine, which labeled GSP terminal fields, did not require further processing.

Confocal Microscopy and Analyses of Terminal Fields.

Imaging. Terminal fields were imaged using a Nikon 80i microscope fitted with a Nikon C2 scanning system (Nikon Instruments, Inc., Melville, NY) and a 10X objective (Nikon, CFIPlanApo; NA=0.45). The nerve labels were matched for the wavelengths of the three lasers in the system (argon laser - 488 nm, 10 mW, IX; DPSS laser - 561 nm, 10mW,

GSP; Modulated Diode laser - 638 nm, 20 mW, CT). Sequential optical sections were captured every 3µm for each 50µm section. Images were obtained with settings adjusted so that pixel intensities were near (but not at) saturation. A transmitted light image at 4X (Nikon PlanFluor; NA=0.13) and at 10X was captured for every physical section containing the labeled terminal field. This permitted an accurate registration of dorsal to ventral brainstem sections among animals using common brainstem landmarks (4X), and identification of NST borders (10X). Group assignment for each set of confocal stacks/mouse was blind to the investigator thresholding the images.

Analyses of Total Terminal Field Volume. Methods used to analyze terminal field volumes and densities were described previously in detail (Sun et al., 2015; Sun et al., 2017). Briefly, quantification of terminal field volume was achieved through the use of custom ImageJ-based software. Each image stack was initially rotated so that the solitary tract was oriented vertically. The border of the NST was outlined for each physical section through the use of the corresponding transmitted light image, and the stack was then cropped to include only the NST. The IsoData thresholder algorithm (Ridler and Calvard, 1978) was applied to yield a binary image stack of the labeled pixels above threshold, and a particle analysis was then performed to quantify the pixel area above threshold for each channel. Volumes from each physical section were summed to yield the total terminal field volume for each mouse. The resultant volume represents an unbiased experimenter measure of the amount of label. Additionally, the volume of colocalization between the terminal fields of two nerves (CT with GSP, GSP with IX, CT with IX) and among all three nerves (CT, GSP, and IX) was determined in a similar manner as described for each single label.

We chose to include axons (e.g., the solitary tract) along with the terminal fields for all animals in our analyses because of the difficulty in accurately deleting these elements from each optical section. Accordingly, the absolute volumes that we show here include the composite terminal field and axons. Since there is no obvious reorganization of nerve tracts among groups, we make the assumption that including the solitary tract in our measurements had a similar quantitative effect among groups.

Analyses of Terminal Field Volume and Density of Labels in Dorsal-Ventral Zones. The analyses of terminal field volumes and density here is the same as was done to study the role of *Bdnf* overexpression in the tongue on terminal field organization in the NST (Sun et al., 2015). The NST was subdivided into X, Y, and Z planes to help identify where terminal field organization of each nerve and the overlaps with other terminal fields occurred. For the medial-lateral and rostral-caudal analyses (X and Y), the NST in the horizontal plane was subdivided into a grid consisting of uniform boxes of 100 pixels X 100 pixels. The NST was aligned relative to the grid, with the intersection of the most medial and most rostral borders of the NST as the 0,0 coordinate.

For analyses in the dorsal-ventral planes (Z), we examined the volume of labeled terminal field in four dorsal-ventral zones and followed the method detailed in Sun et al., (2015). Briefly, in horizontal sections, we subdivided the NST into four zones -- Far Dorsal, Dorsal, Intermediate and Ventral Zones (see Sun et al., 2015 for definitions of zones). The landmarks used to define each zone were consistent among the groups. To check for reliability, a person naïve to previous assignment of sections into zones assigned sections for each animal into the 4 zones. With minor exceptions, the dorsal-ventral zone assignments among investigators were the same.

Density by Dorsal – Ventral Zones. Density measures were not statistically analyzed, but were qualitatively examined through heat maps for each dorsal-ventral zone containing a 5 X 10 (column X row) grid.

Examination of Terminal Fields in Coronal Sections. The NST from two UBC-*Bdnf* iKO No TAM mice (females, > 90 days old) and two UBC-*Bdnf* iKO mice (females, > 90 days old) were sectioned coronally on a vibratome at 50µm and imaged as described above. Coronal sections were used to examine the extent of terminal field expansion and overlapping fields in the NST. No quantitative measurements were taken. Coronal sections were also imaged with transmitted light to allow visualization of NST and brainstem landmarks to qualitatively compare terminal field labels among sections in the same rostral-caudal plane.

Geniculate Ganglion and Petrosal Ganglion Cell Number. All mice were at least 3 months old. The CT (UBC-*Bdnf* iKO No TAM, n=4: 2 males, 2 females; UBC-*Bdnf* iKO, n=8: 4 males, 4 females) or the GSP (UBC-*Bdnf* iKO No TAM: n=5, 2 females, 3 males; UBC-*Bdnf* iKO: n=5, 2 males, 3 females) nerve was labeled as described for the terminal field labeling procedure, with the exception that the 3 kD tetramethylrhodamine dextran was chosen as the only tracer because it did not require further processing for visualization. This allowed imaging the entire intact ganglion, thereby allowing us to count all labeled cells. Petrosal ganglia (UBC-*Bdnf* iKO No TAM: n=4, 2 males, 2 females; UBC-*Bdnf* iKO: n=9, 6 males, 3 females) were also labeled by way of the IX, using the tetramethylrhodamine tracer. Ganglia collection, processing and imaging were similar to that described in Sun et al. (2015; 2017).

CT Nerve Neurophysiology. All animals used for taste recording experiments were at least 3 months old. Mice (Controls; n = 8: 4 males, 4 females; K14-*Bdnf* iKO No TAM; n = 6: 3 males, 3 females; K14-*Bdnf* iKO, n = 5: 2 males, 3 females; UBC-*Bdnf* iKO No TAM; n = 6: 3 males, 3 females; UBC-*Bdnf* iKO, n = 6: 4 males, 2 females) were anesthetized as described for the "Fluorescent Anterograde Nerve Labeling" procedure. Procedures for recording taste responses from the CT and data analyses were as described by Sun et al. (2015; 2017) and are only briefly described here. Taste responses were recorded to an ascending concentration series of 0.05, 0.1, 0.25, and 0.5 M NaCl, 10, 20, and 50 mM citric acid, 0.1, 0.25, 0.5 and 1.0M sucrose, and 10, 20, 50, and 100 mM quinine hydrochloride. All chemicals were reagent grade and prepared in artificial saliva (Hellekant et al., 1985). Each concentration series was bracketed by applications of 0.5M NH_4Cl to monitor the stability of each preparation and for normalizing taste responses. Solutions were applied to the tongue in 5 ml aliquots with a syringe and allowed to remain to the tongue for ~20 sec. After each solution application, the tongue was rinsed with artificial saliva for $\geq$1 min. when the stimulus concentration was high. This period allows for full recovery of neural responses (i.e., the responses were not adapted by previous responses) (Shingai and Beidler, 1985). CT responses were calculated as follows: the average voltage of the spontaneous activity that occurred for the 5 secs before stimulus onset was subtracted from the average voltage that occurred from the period from the 5^{th} to 15^{th} sec after stimulus application. Response magnitudes were then expressed as ratios relative to the mean of 0.5M NH_4Cl responses before and after stimulation. Whole nerve response data were retained for analysis only when 0.5M NH_4Cl responses that bracketed a concentration series varied by <10%. In addition,

responses were recorded to the NaCl concentration series in the epithelial sodium channel blocker, amiloride (50 μM) (Benos, 1982). Rinses during this series were with amiloride.

Experimental Design and Statistical Analysis.

qPCR Results: Means of normalized *Bdnf* expression levels were compared between K14-*Bdnf* iKO No TAM and K14-*Bdnf* iKO mice for anterior tongue, geniculate ganglion and NST with a two-tailed unpaired t test. The same analysis was also done between UBC-*Bdnf* iKO No TAM and UBC-*Bdnf* iKO mice.

Terminal Field Volumes: The mean (± SEM) was calculated for the total CT, GSP, and IX nerve terminal field volumes, for their overlapping field volumes, and for terminal field volumes within the four, defined dorsal-ventral zones. We first analyzed the terminal fields by comparing volumes among the three nerves (i.e., IX, CT, GSP). We then separately analyzed terminal fields by comparing the overlaps among the nerves (e.g., CT with GSP). This was done through a 2-way Analysis of Variance (SPSS, ANOVA; RRID: SCR_002865; experimental group X nerve/overlap), with post-hoc pairwise comparisons done with Bonferroni post-tests (SPSS). For all statistical tests, we considered p values ≤ 0.05 to be significant.

Ganglion Cell Counts: Ganglion cell numbers for the CT, GSP and IX were compared among controls, K14-*Bdnf* iKO mice and UBC-*Bdnf* iKO mice and analyzed with a 2-way Analysis of Variance (SPSS; ANOVA; experimental group X nerve), with post-hoc pairwise comparisons done with Bonferroni post-tests (SPSS). For all statistical tests, we considered p values ≤ 0.05 to be significant.

Whole-Nerve Taste Responses: A 2-Way Repeated Measures ANOVA (SPSS) was used to compare mean ($\pm$ SEM) relative CT responses (compared to 0.5M NH_4Cl responses)

initially among control, K14-*Bdnf* iKO No TAM, and K14-*Bdnf* iKO mice, and then among control, UBC-*Bdnf* iKO No TAM, and UBC-*Bdnf* iKO mice to a concentration series of NaCl, sucrose, citric acid, and quinine hydrochloride (each -- 3 groups X 3 or 4 concentrations. Post-hoc pairwise comparisons done with Bonferroni post-tests). For all statistical tests, we considered p values ≤ 0.05 to be significant.

RESULTS

Bdnf mRNA Expression is Selectively Reduced in the Tongue of K14-Bdnf iKO Mice and Reduced in the Tongue, Geniculate Ganglion and NST in UBC-Bdnf iKO Mice Following Tamoxifen.

K14-Bdnf iKO mice. *Bdnf* expression in mice that had the gene deleted on one allele throughout development (K14-*Bdnf* iKO No TAM mice) showed an approximate 32% decrease in the amount of expression in tongue compared to the control standard (control=1.0; Fig. 1A). By contrast, tamoxifen administration at adulthood in K14-*Bdnf* iKO mice resulted in an 88% decrease in *Bdnf* expression in the tongue at 2 months after the treatment compared to controls (Fig. 1A). This decrease in *Bdnf* expression was significantly more than found in K14-*Bdnf* iKO No TAM mice ($t(11)=19.7$; $p=0.0001$). The amount of *Bdnf* expression in the geniculate ganglion for K14-*Bdnf* iKO No TAM and K14-*Bdnf* iKO mice decreased approximately 30% and 27% below controls, respectively (Fig. 1B). A similar pattern of expression was apparent in the NST. In this structure, the amount of *Bdnf* expression decreased 30% and 23% in K14-*Bdnf* iKO No TAM and K14-*Bdnf* iKO mice, respectively, from the control standard (Fig. 1C). There were no significant differences in expression between these two groups for geniculate

ganglion or NST (t(8)=0.2; p=0.87 and t(8)=0.6; p=0.56, respectively). Therefore, *Bdnf* expression levels were dramatically and selectively reduced in the tongue at adulthood.

UBC-Bdnf iKO mice. Our goal for experiments in this group of mice was to inducibly reduce *Bdnf* expression significantly at adulthood in all tissues. We found, for all three tissues, that *Bdnf* expression was drastically decreased in UBC-*Bdnf* iKO mice at 2-months post tamoxifen. In the tongue, UBC-*Bdnf* iKO No TAM mice showed a decrease of approximately 34% compared to controls; whereas, there was a 90% decrease in *Bdnf* expression in UBC-*Bdnf* iKO mice compared to controls (Fig. 1D). The mean expression in the anterior tongue was significantly different between UBC-*Bdnf* iKO No TAM and UBC-*Bdnf* iKO mice (Fig. 1D) (t(10)=13.0; p=0.0001). Similarly, the amount of *Bdnf* expression was successively decreased in UBC-*Bdnf* iKO No TAM and in UBC-*Bdnf* iKO mice in both the geniculate ganglion and NST (Fig. 1E,F). Specifically, *Bdnf* expression decreased by 25% and 92% in the geniculate ganglia of UBC-*Bdnf* iKO No TAM and UBC-*Bdnf* iKO mice, respectively (comparison between groups: (t(5)=9.4; p=0.0002), and decreased by 30% and 94% in the NST of UBC-*Bdnf* iKO No TAM and UBC-*Bdnf* iKO mice, respectively (comparison between groups: (t(6)=9.4; p=0.0001).

The differences in expression of *Bdnf* in the geniculate ganglion and NST between K14-*Bdnf* iKO and UBC-*Bdnf* iKO mice can be explained by the different sites where *Bdnf* was deleted. Unlike K14-*Bdnf* iKO mice, where *Bdnf* was only deleted in the tongue, it was deleted in tongue, geniculate ganglion, and NST in UBC-*Bdnf* iKO mice. All three of these structures normally express *Bdnf* (Conner et al., 1997; Meng et al., 2015). We also found *Bdnf* expression in the NST at locations corresponding to the gustatory recipient zone for the three nerves (data not shown). Although we did not

measure *Bdnf* expression in the petrosal ganglion (cell soma of the IX), these cells also express *Bdnf* (Brady et al., 1999). Thus, it is likely that *Bdnf* was deleted in these cells also.

The Rostral NST in UBC-Bdnf iKO Mice Shows Less Immunoreactivity to BDNF Antibodies Than in Control Mice.

To test if our *Bdnf* expression data from the NST were reflected in immunoreactivity for BDNF, we qualitatively examined immune-stained tissue in two control and two UBC-*Bdnf* iKO mice. Figure 1G shows that there was robust immuno-positive labeling in the rostral NST in control mice. The NST in UBC-*Bdnf* iKO mice lack the punctate labeling seen in controls and only showed background staining (Fig. 1G). Interestingly, there was noticeably more immune-positive staining in the rostral NST in controls compared to adjacent regions in the brainstem (Fig. 1G).

Total Terminal Field Volumes are Enlarged Differentially in Mice Where Bdnf Expression was Reduced in the Tongue or in All Tissues.

Control Mice. Similar to what was found for control mice in a study where *Bdnf* was overexpressed in the tongue (Sun et al., 2015), the total terminal field volumes for all three nerves (IX, CT, GSP) in controls were similar to each other (Fig. 2A; black bars). Moreover, the total terminal field size for double (CT with GSP; IX with GSP, IX with CT) and the triple terminal field (CT with GSP with IX) overlaps were similar in size to control mice in the Sun et al. (2015) study (Fig. 2A; black bars).

Bdnf iKO No TAM mice. As noted earlier, two additional control groups had all of the transgenes for K14-*Bdnf* iKO or for UBC-*Bdnf* iKO but did not receive administration of tamoxifen (No TAM). The terminal field volumes for these two groups were similar to

each other ($p > 0.05$); therefore, we pooled these data into one control group denoted as *Bdnf* iKO No TAM mice (Fig. 2A). This group represents the effects of the *Bdnf* knockout on a single allele throughout development. For all total terminal field volumes, the *Bdnf* iKO No TAM mice were statistically similar to littermate controls that lacked all of the transgenes (Fig. 2A; blue bars; Table 1; all posttests $p>0.1$).

Total Terminal Field Volumes in Mice Where Bdnf Expression Was Reduced in the Tongue.

In contrast to control mice, the CT and GSP terminal field volumes in mice in which *Bdnf* expression was significantly reduced in the tongue were greater than found for the IX. Moreover, the total terminal field volumes for the CT and GSP in K14-*Bdnf* iKO mice were 48% and 81% greater, respectively, than the total terminal field volumes found in controls (Fig. 2A; Table 1; posttest p values = 0.004 and 0.0001, respectively) and 61% and 86% greater, respectively, than in *Bdnf* iKO No TAM mice (Fig. 2A; Table 1; posttest p values = 0.003 and 0.0001, respectively). Furthermore, the CT with GSP overlapping field volumes in K14-*Bdnf* iKO mice was 69% greater than in control mice (Table 1; posttest p value = 0.0001) and 105% greater than in *Bdnf* iKO No TAM mice (Table 1; posttest p value = 0.0001). All other terminal field sizes (IX and other overlapping fields) in K14-*Bdnf* iKO mice were similar to those in control and in *Bdnf* iKO No TAM mice (Fig. 2A; Table 1; range of posttest p values = 0.16 – 1.00).

Total Terminal Field Volumes in Mice Where Bdnf Expression Was Reduced in All Cells.

In contrast to mice in which *Bdnf* expression was significantly reduced only in the tongue at adulthood, large-scale increases in total terminal field volumes were apparent when *Bdnf* expression was reduced in all cells. Specifically, the total terminal field size

for the IX, CT, and GSP nerves in UBC-*Bdnf* iKO mice were 121%, 100%, and 77% greater than the respective terminal field volumes in control mice (Fig. 2A; Table 1; posttest p values = 0.0001, 0.0001, and 0.002, respectively) and 81%, 118%, and 83% greater than the respective terminal field volumes in *Bdnf* iKO No TAM mice (Fig. 2A; Table 1; posttest p values = 0.0001, 0.0001, and 0.001, respectively). Moreover, all of the overlapping fields were approximately 2X the total volume of the respective fields of overlap found in control mice (Fig. 2A; Table 1; posttest p value range = 0.01 – 0.0001) and 2X to 2.5X the total volume of the respective fields of overlap found in *Bdnf* iKO No TAM mice (Fig. 5; Table 1; posttest p value range = 0.001 – 0.0001).

Total Terminal Field Volume Differences Between K14-Bdnf iKO and UBC-Bdnf iKO Mice.

To further examine the role of BDNF in the organization of terminal fields in the rostral NST, we examined differences between the two tamoxifen-treated groups. As seen in Figure 2A, the terminal field volumes for the IX and CT in mice in which *Bdnf* expression was reduced in all cells were significantly larger (71%, IX; 36%, CT) than in mice where *Bdnf* expression was reduced only in the tongue (Table 1; posttest p values = 0.0001). As could be expected from the terminal field volumes of the nerves, the IX with CT overlapping field volumes in UBC-*Bdnf* iKO mice were nearly 2X greater than that in K14-*Bdnf* iKO mice (Fig. 2A; Table 1; posttest p = 0.0001). No other group-related comparisons were significant (posttest p value range = 0.19 – 1.00).

Total Terminal Field Volume Summary.

Removal of *Bdnf* from the tongue at adulthood had effects on the total terminal field volumes of the CT and GSP within 2 months after tamoxifen administration. In

contrast, removal of *Bdnf* from all cells had a global effect on all terminal field volumes by significantly increasing them relative to controls. Moreover, the lack of the *Bdnf* gene on one allele throughout development had no effect on total terminal field volumes.

Terminal Field Volumes and Densities Within NST Dorsal-Ventral Zones.

Expansion of the Terminal Fields Volumes Occurs in Multiple Dorsal-Ventral Zones.

To test if the terminal fields of experimental mice were reorganized in one or more dorsal-ventral zones in the NST, we examined differences in terminal field volumes in each of the four dorsal to ventral zones described earlier.

Far Dorsal Zone

For all groups, this zone contained the least volume of terminal field labeling (Fig. 2B; note difference in Y axis compared to Figs. 2C-E). Moreover, the far dorsal zone had more IX terminal field labeling than that for the CT and GSP (Fig. 2B). However, the only significantly differences in terminal field volumes among groups were that the IX terminal field volume in UBC-*Bdnf* iKO was approximately 3X and 2X greater than controls and *Bdnf* iKO No TAM mice, respectively (Fig. 2B; Table 1; posttest p values = 0.0001 and 0.005, respectively). For overlapping fields, the IX with CT overlap volume for UBC-*Bdnf* iKO mice was 4X greater than in controls (posttest p value = 0.0001), 5X greater than in *Bdnf* iKO No TAM mice (posttest p value = 0.0001), and 1.6X greater than in K14-*Bdnf* iKO mice (posttest p value = 0.001) (Fig. 2B; Table 1). No other significant differences were found for this zone.

Dorsal Zone

As in the Far Dorsal Zone, the IX terminal field volume was 1.6X and 2X greater than in controls and *Bdnf* iKO No TAM mice, respectively (posttest p values = 0.03 and

519 0.002, respectively). It was also 1.5 X greater than in K14-*Bdnf* iKO mice (Fig. 2C; Table
520 1; posttest p value = 0.05). Unlike that seen in the Far Dorsal Zone, the CT terminal field
521 volume in K14-*Bdnf* iKO and UBC-*Bdnf* iKO mice were greater than the two control
522 groups. For K14-*Bdnf* iKO mice, the CT terminal field volume was approximately 2X
523 and 3.5X greater than in controls and in *Bdnf* iKO No TAM mice, respectively (Fig. 2C,
524 Table 1; posttest values = 0.05 and 0.02, respectively). For UBC-*Bdnf* iKO mice, the CT
525 terminal field volume was approximately 2.7X and 4.8X greater than in controls and in
526 *Bdnf* iKO No TAM mice, respectively (Fig. 2C, Table 1; posttest values = 0.01 and
527 0.001, respectively). Finally, the terminal field overlap volume between the IX and CT
528 for UBC-*Bdnf* iKO mice was 4.8X greater than in controls (posttest p value = 0.0001),
529 7.7X greater than in *Bdnf* iKO No TAM mice (posttest p value = 0.0001), and 1.9X
530 greater than in K14-*Bdnf* iKO mice (posttest p value = 0.03) (Fig. 2C; Table 1). No other
531 significant differences were found for this zone.

532 **Intermediate Zone**

533 This zone had similar proportions of terminal field labeling for the IX, CT and
534 GSP within each of the four groups (Fig. 2D). Moreover, the pattern of terminal field
535 volume differences described for the Dorsal Zone occurred here also. That is, group-
536 related differences in terminal field volumes were apparent for the IX, CT and IX with
537 CT terminal field overlap (Fig. 2D). The only difference between the two zones was that
538 the CT volume in UBC-*Bdnf* iKO mice was different than all of the other three groups
539 (Fig. 2D). In this zone, the terminal field volume for the IX in UBC-*Bdnf* iKO mice was
540 approximately 1.4X – 2X greater than in the other three groups (Fig. 2D; Table 1;
541 posttest p value range = 0.006 – 0.05), the CT was approximately 1.5X greater than in the

other three groups (Fig. 2D; Table 1; posttest p values = 0.01 – 0.05), and the IX with CT overlap terminal volume was approximately 2X greater than in the other three groups (Fig. 2D; Table 1; posttest p value range = 0.07 – 0.04). No other significant differences were found for this zone.

Ventral Zone

For all groups, this zone contained the least amount of IX terminal field volume, and there were no significant differences among groups for the IX. Thus, the group-related differences in this zone were confined to the CT, GSP, and CT with GSP overlap terminal field volumes (Fig. 2E). For the CT, GSP, and CT with GSP overlaps, both K14-*Bdnf* iKO and UBC-*Bdnf* iKO mice had significantly greater (1.5X – 3X) terminal field volumes than in controls (Fig. 2E; Table 1; posttest p value range = 0.0001 – 0.03) and *Bdnf* iKO No TAM mice (Fig. 2E; Table 1; posttest p value range = 0.0001 – 0.02). No other significant differences were found for this zone.

Summary of Terminal Field Volumes Across Zones.

Group-related differences for terminal field volumes occurred through all dorsal-ventral zones, but less so in the Far Dorsal Zone because of the relatively small amount of label for all nerves. Moreover, UBC-*Bdnf* iKO mice showed the most differences in terminal field volumes from controls and occurred in all three nerves distributed among all four zones.

Group-Related Terminal Field Changes Occur in the Densest Regions of the NST Normally Occupied in Controls.

To test if the group-related differences in terminal field volumes represent a spatial reorganization of the respective terminal fields, we qualitatively examined

565 representative photomicrographs and examined density plots of the IX, GSP, CT and
566 triple overlap terminal field volumes in each zone for *Bdnf* iKO No TAM, K14-*Bdnf*
567 iKO, and UBC-*Bdnf* iKO mice (Fig. 3). For clarity, we chose not to show data from
568 Control mice in Figure 3 because they were qualitatively similar to *Bdnf* iKO No TAM
569 mice.

570 **Far Dorsal Zone**

571 The terminal field volume differences shown in Figure 2B were reflected in
572 photomicrographs of terminal fields from this zone (Fig. 3A). That is, the largest amount
573 of IX labeling is evident in the photomicrograph for the UBC-*Bdnf* iKO mouse, followed
574 by labeling in the K14-*Bdnf* iKO, and finally in the *Bdnf* iKO No TAM mouse.
575 Moreover, it appears that the fields for the IX, GSP, and CT were not drastically
576 rearranged in the two experimental groups. That is, the same pattern of innervation
577 occurred among the *Bdnf* iKO No TAM, K14-*Bdnf* iKO, and UBC-*Bdnf* iKO mice (Fig.
578 3A), and is reflected in the group measures of terminal field densities within the NST
579 (Fig. 3B). For the density measures shown in Figure 3B, the primary characteristic that
580 distinguishes differences among the three groups was the amount of label within specific
581 locations containing the densest label within each group (Fig. 3B). The densest region of
582 terminal fields (or "core" of labeling) for each group was approximately at the same
583 location across the three groups for each nerve, but with the densest label across all
584 nerves and for the triple overlap located at the "core" region for the IX in UBC-*Bdnf* iKO
585 mice (see white rectangle in Fig. 3B).

586 **Dorsal Zone**

As noted for the far dorsal zone, the terminal field distribution was similar among groups for each nerve and differences in amount of labeling in the same location is consistent with the differences in terminal field volumes (Fig. 3A). In this zone, however, there was also an extension of terminal field beyond the densest projection in the K14-*Bdnf* iKO and UBC-*Bdnf* iKO mice compared to controls. This is especially apparent in the density representations between *Bdnf* iKO No TAM and UBC-*Bdnf* iKO mice (Fig. 3B). As seen in the Far Dorsal Zone, the densest region among all nerves and across all three groups was for the IX in UBC-*Bdnf* iKO mice (Fig. 3B).

Intermediate Zone

The photomicrographs from this zone clearly shows a greater amount of IX, GSP, and CT labeling in UBC-*Bdnf* iKO mice compared to *Bdnf* iKO No TAM mice. However, as in the other zones, the location of labels was similar among the three groups (Fig. 3A). The amount of terminal field labeling in the K14-*Bdnf* iKO mouse was intermediate to the other two groups (Fig. 3A). These terminal field characteristics are also evident in the density measurements (Fig. 3B). Unlike the other zones, the location of the greatest amount of labeling occurred for the GSP in UBC-*Bdnf* iKO mice, although it was not much greater than the respective location of CT label in UBC-*Bdnf* iKO mice (Fig. 3B).

Ventral Zone

Here, as shown in Figure 2E, there was relatively little terminal field label of the IX compared to GSP and CT labels for all groups. Also, while there was more terminal field volume for the GSP and CT in K14-*Bdnf* iKO and UBC-*Bdnf* iKO mice compared to that in *Bdnf* iKO No TAM mice (Fig. 2E), the photomicrographs (Fig. 3A) and density

analyses (Fig. 3B) indicate that the difference in volume is likely due to spread of label beyond the densest region of the NST. That is, similar amounts of labeling within each nerve and for the triple overlap occurred among all groups in the "core" region, but with more spread of label laterally in K14-*Bdnf* iKO and UBC-*Bdnf* iKO mice compared to *Bdnf* iKO No TAM mice (Fig. 3B). As noted for the Intermediate Zone, the location of densest labeling among all nerves and groups in this zone occurred for the GSP in UBC-*Bdnf* iKO mice (Fig. 3B).

More Terminal Field Labeling is Also Seen in Coronal Sections from UBC-Bdnf iKO Mice.

Figure 4 shows coronal sections of terminal fields of the three nerves (Fig. 4A,C,E, for the IX, GSP, and CT, respectively in a UBC-*Bdnf* iKO No TAM mouse, B,D,F for the IX, GSP, and CT, respectively in a UBC-*Bdnf* iKO mouse) and their triple overlap (Fig. 4G in a UBC-*Bdnf* iKO No TAM mouse, H in a UBC-*Bdnf* iKO mouse). The section shown in Figure 4 is approximately 200 µm caudal to the anterior pole of the NST (Fig. I,J), which corresponds to the Ventral Zone of the NST noted in Figures 2 and 3. Here, there is little IX labeling compared to the GSP and CT in the UBC-*Bdnf* iKO No TAM mouse. By comparison, in the UBC-*Bdnf* iKO mouse shown, there is more IX labeling than would be expected from the terminal field volume data (Fig. 3D) and significant amounts of GSP and CT labels. The photomicrographs support the conclusions drawn from Figure 3 in that the primary group-related differences in GSP and CT terminal field labels occur in the "core" region of the fields and not a significant rearrangement of the fields.

Ganglion Cell Counts of the CT, GSP, and IX.

Since BDNF plays a significant role in cell death of neurons (Levi-Montalcini and Angeletti, 1963), we were interested to find if loss of BDNF at adulthood resulted in a loss of neurons in the peripheral gustatory system. We counted the number of neurons in the geniculate ganglion that made up the CT and GSP nerves, and in the petrosal ganglion that made up the IX.

In control mice, the number of geniculate ganglion cells that made up the CT were similar to those of the GSP (Mean ± SEM: CT, 210.0 ±18.3; GSP, 196.0 ± 11.0) and both were significantly less than (Table 1; posttest p values = 0.0001) the number of petrosal ganglion cells that made up the IX (IX, 307.2 ± 4.8). The differences in cell numbers between the two ganglia likely relates to the size of the respective nerves, the relative greater field size of innervation by the IX, and relative differences in the type of sensory neurons (i.e., taste vs mechanosensory) (Frank, 1991). The same pattern of ganglion cell numbers also occurred in K14-*Bdnf* iKO mice (CT, 212.0 ± 8.0; GSP, 190.2 ± 7.3; IX, 311.7 ± 12.7) and in UBC-*Bdnf* iKO mice (CT, 193.8 ± 7.6; GSP, 191.0 ± 9.1; IX, 279.2 ± 4.0). For these experimental groups, the number of CT and GSP neurons were significantly less than the respective number of IX ganglion cell neurons (Table 1; posttest p values = 0.0001). There were no group-related differences in ganglion cell counts for any of the three nerves (Table 1; p value range = 0.57 – 1.000). Therefore, deletion of *Bdnf* from either the tongue or from all cells at adulthood did not impact the number of ganglion cells that represent the CT, GSP or IX.

Neurophysiological Taste Responses in the CT.

To test if the terminal field volume changes that we see here may be due to activity-dependent alterations in the function of at least one of these nerves, we recorded

656 whole-nerve taste responses from the CT to an array of taste stimuli. Such a hypothesis
657 is driven by the decreased innervation of taste buds on the anterior tongue when *Bdnf* was
658 removed from the gustatory system at adulthood (Meng et al., 2015), and the
659 demonstrated role of taste-elicited activity on the development and maintenance of these
660 terminal fields (Skyberg et al., 2017; Sun et al., 2017). Surprisingly, there were no
661 significant differences among taste responses among control, K14-*Bdnf* iKO No TAM,
662 and K14-*Bdnf* iKO mice (Tables 1 & 2; Fig. 5; posttest p value range = 0.07 – 1.00; 52%
663 of comparisons p = 1.00) to any concentration of any stimulus. Similarly, with the
664 exception of one posttest comparison, there were no significant differences among taste
665 responses from control, UBC-*Bdnf* iKO No TAM, and UBC-*Bdnf* iKO mice (Tables 1 &
666 2; Fig. 5; posttest p value range = 0.04 – 1.00l; 74% of comparisons p = 1.00). The only
667 significant difference between mean relative responses (total posttest comparisons = 114)
668 was to 0.5M NaCl after amiloride application. The responses in UBC-*Bdnf* iKO No TAM
669 mice were significantly less than in controls (Fig. 5; posttest p = 0.04). We do not regard
670 this difference as biologically significant because it involves two control groups and the
671 means are small, with a relatively small difference between them (Fig. 5). Collectively,
672 these findings strongly indicate that the arborizations of the CT, particularly in the taste
673 bud, do not translate to functional taste response changes in this nerve.

674 **DISCUSSION**

675 Deleting *Bdnf* in the tongue or in all tissues at adulthood resulted in an expansion
676 of the terminal fields of gustatory nerves as they made their central contacts in the NST.
677 We show here that deleting *Bdnf* in all tissues had more widespread effects on terminal
678 field organization than if deleted only in the tongue. Thus, the maintenance of gustatory

679 terminal field organization at adulthood requires normal expression of *Bdnf* in the
680 peripheral targets of taste nerves, taste buds, and is exaggerated when *Bdnf* is removed
681 from other tissues. These effects are not due to changes in numbers of neurons or to
682 changes in whole nerve taste responses from the CT.

683 **Deleting *Bdnf* at Adulthood has Opposite Effects on Maintenance of Axonal**
684 **Branching of Peripheral Processes Compared to Central Processes.**

685 The expansion of terminal fields is especially surprising because similar
686 experimental treatments as those used here produced decreased branching of the CT in
687 the tongue (Meng et al., 2015). Thus, the peripheral process of the CT decreases in
688 branching while the central process of the same nerve expands when *Bdnf* is deleted at
689 adulthood. Meng et al. (2015) showed that inducibly deleting *Bdnf* in the tongue or in all
690 tissues in adult mice with the same genetic strategy used here resulted in an approximate
691 40% loss of innervation, a 30% decrease in taste bud cells size and in taste cell numbers,
692 without a loss of neurons or taste buds. These effects were attributed, in part, to
693 deficiencies in nerve/target (i.e., CT/taste bud) matching (Meng et al., 2015). Briefly,
694 taste bud cells produce BDNF during development to recruit incoming axons (Nosrat et
695 al., 1996; Nosrat et al., 2001; Hoshino et al., 2010; Huang and Krimm, 2010). BDNF
696 production continues into adulthood (Yee et al., 2003), which likely maintains normal
697 taste bud morphology and numbers (Farbman, 1969; Cheal and Oakley, 1977; Whitehead
698 et al., 1987; Guagliardo and Hill, 2007) during the lifelong renewal of taste bud cells
699 (Beidler and Smallman, 1965). Therefore, deleting *Bdnf* in the tongue at adulthood leads
700 to the loss of a critical factor that maintains normal, mutual interactions between taste
701 buds and their innervating neurons.

The Central Effects of *Bdnf* Deletion are Unusual in Their Effects.

Our finding here that terminal fields are expanded in the NST in mice where *Bdnf* is deleted at adulthood, suggests different mechanisms operate at both ends of the same nerve. Moreover, this increase in size of the central projections does not match what may be expected from many other studies that examine the role of BDNF on axonal arbors and dendritic structures.

In addition to a key feature of neurotrophins to support neuronal survival during early development (Levi-Montalcini and Hamburger, 1951; Levi-Montalcini and Cohen, 1956; Levi-Montalcini and Angeletti, 1963), they also impact the architecture of axonal arbors and dendritic structure during development as well as maintaining pre- and post-synaptic structures. Such roles have been identified for BDNF. An excess of this neurotrophin produces more complex and longer axonal arbors in projecting neurons during development (Davies et al., 1986; Cohen-Cory and Fraser, 1995; Huang and Reichardt, 2001; Poo, 2001; Cohen-Cory et al., 2010) and at adulthood (Thanos et al., 1989), and increases in the number of synapses on dendrites, dendritic lengths, and branching (Cohen-Cory and Fraser, 1995; Alsina et al., 2001; Cohen-Cory et al., 2010). Conversely, loss of BDNF and/or its receptor, TrkB, often results in a paring back of the terminal fields (Cohen-Cory, 1999). Given these findings, we would predict smaller instead of expanded terminal fields when *Bdnf* was deleted. However, there is an important finding from studies in the *Xenopus* visual system that may inform our results. In the *Xenopus* retinotectal pathway, BDNF has opposite effects on the branching of terminal fields in the tectum than it does on retinal ganglion cell dendrites (Lom and Cohen-Cory, 1999; Lom et al., 2002). Thus, the differential spatial effects on branching

of the same neuron are similar to what we and Meng et al. (2015) show in the peripheral gustatory system, and point to the importance of spatially-dependent processes (i.e., peripheral vs central) in determining how axonal processes respond to alterations in *Bdnf* expression.

Lack of "Competition" Among Gustatory Terminal Fields in the NST Produces an Immature Organization.

We are struck by the similarity of terminal field organization in our experimental mice here with that described in multiple experimental studies of the terminal field organization in rodents. In particular, it appears that a diverse set of experimental manipulations leads to a "reversion" to the immature terminal field organization found in early postnatal rats and mice (May and Hill, 2006; Zheng et al., 2014). Briefly, during early development, the CT, GSP, and IX all send extensive and largely overlapping projections to the NST. This organization is then significantly refined in control animals from approximately postnatal P15 to P30, at which age each of the terminal fields occupy distinct and more focused regions in the NST (Mangold and Hill, 2008). The immature terminal field organization is shared with adult rodents that have a history of early or lifelong dietary NaCl manipulations (May and Hill, 2006; Mangold and Hill, 2008; Zheng et al., 2014), deletion of the primary sodium taste transduction pathway during development (Sun et al., 2017) or at adulthood (Skyberg et al., 2017), overexpression of *Bdnf* at inappropriate locations in the tongue throughout development (Sun et al., 2015), and in the CT of rodents that have the GSP and IX cut at adulthood (Corson and Hill, 2011). Our conclusion from these diverse studies is that alterations in the normal "competition" among the three terminal fields (e.g., changes in taste-elicited activity,

amount of innervation) during development or at adulthood leads to a reestablishment of the immature terminal field seen in young control rodents. That is, a lack of competition for factors, which may include neurotrophins, modulatory molecules, and synaptic sites, leads to the expanded terminal field organization (Thoenen, 1995; Singh and Miller, 2005; Singh et al., 2008). One hypothesis, which may more directly relate to the findings here, may be that a decrease in the amount of anterogradely-transported release of BDNF from the terminals (Zhou and Rush, 1996; Conner et al., 1997; Altar and DiStefano, 1998; Fawcett et al., 1998; Tonra et al., 1998; Tonra, 1999) of one or more gustatory nerves, could destabilize taste nerve synapses onto their target NST cells. Findings from rat show that central taste neurons in the NST become less narrowly tuned, but increase in response frequencies (i.e., amplify the taste signal) with age (Hill et al., 1983), suggesting that more synapses from more peripheral neurons are recruited during development. Lack of an organizing signal, such as BDNF, may lead to a disassembly of these circuits that resemble the immature organization. Indeed, evidence from other systems demonstrates that BDNF stabilizes synapses (Hu et al., 2005; Je et al., 2012).

We also suggest that expanded terminal fields in both K14-*Bdnf* iKO and UBC-*Bdnf* iKO mice are due primarily to the reduced amount of anterogradely-transported, taste bud-derived BDNF. The additive *Bdnf* deletion in ganglia and NST may explain the exaggerated effects seen in UBC-*Bdnf* iKO mice. Obviously, this hypothesis is speculative and requires more careful, mechanistic investigations that will enable an explanation of the significant amount of plasticity of these terminal fields during development and at adulthood.

Implications for Central Taste Function and Taste-Related Behaviors.

Our findings that functional CT taste responses are not affected in mice with *Bdnf* deletion is surprising, given there are significant group-related differences in axonal branching and numbers of taste bud cells (Meng et al., 2015). However, a recent report in which taste buds were removed pharmacologically, showed that CT relative taste responses were intact even with an approximate 50% decrease in the number of taste buds (Kumari et al., 2017). This not only supports our functional data, but also illustrates how resilient the peripheral gustatory system is in sending stimulus-specific information to the brain. Nonetheless, because we can only analyze relative response magnitudes from whole nerves (Beidler, 1953), there may be an overall decrease in afferent activity in our experimental animals that could influence activity-dependent processes impacting synapse formation and stabilization. Regardless of the mechanism(s), our findings of the enlarged terminal fields strongly indicate that functional changes in the central gustatory circuitry likely occur. For example, if more functional synapses accompany the increase terminal field volumes, there may be a broadening of gustatory information received by single NST neurons. This would potentially lead to significant changes in coding of taste quality and concentration at the first central relay. In turn, the deletion of *Bdnf* at adulthood could also lead to significant behavioral consequences, including alterations in taste thresholds, taste discrimination, and taste-related ingestive behaviors.

In short, we show that the maintenance of the adult mouse central gustatory system is especially plastic and dependent on *Bdnf* expression in the tongue and in other tissues. As such, it is an ideal system to study circuit plasticity at adulthood and the role of neurotrophins in controlling neuronal structure and function.

794 **References**

796

797 Alsina B, Vu T, Cohen-Cory S (2001) Visualizing synapse formation in arborizing optic
798 axons in vivo: dynamics and modulation by BDNF. Nat Neurosci 4:1093-1101.

799 Altar CA, DiStefano PS (1998) Neurotrophin trafficking by anterograde transport Trends
800 Neurosci 21:433-437.

801 Bartel DL, Finger TE (2013) Reactive microglia after taste nerve injury: comparison to
802 nerve injury models of chronic pain. F1000Research 2:65.

803 Beidler LM (1953) Properties of chemoreceptors of tongue of rat. Journal of
804 neurophysiology 16:595-607.

805 Beidler LM, Smallman RL (1965) Renewal of cells within taste buds. Journal of Cell
806 Biology 27:263-272.

807 Benos DJ (1982) Amiloride: a molecular probe of sodium transport in tissues and cells.
808 Am J Physiol 242:C131-145.

809 Brady R, Zaidi SI, Mayer C, Katz DM (1999) BDNF is a target-derived survival factor
810 for arterial baroreceptor and chemoafferent primary sensory neurons. J Neurosci
811 19:2131-2142.

812 Cheal M, Oakley B (1977) Regeneration of fungiform taste buds: temporal and spatial
813 characteristics. J Comp Neurol 172:609-626.

814 Cohen-Cory S (1999) BDNF modulates, but does not mediate, activity-dependent
815 branching and remodeling of optic axon arbors in vivo. J Neurosci 19:9996-
816 10003.

817 Cohen-Cory S, Fraser SE (1995) Effects of brain-derived neurotrophic factor on optic
818 axon branching and remodelling in vivo. Nature 378:192-196.

819 Cohen-Cory S, Kidane AH, Shirkey NJ, Marshak S (2010) Brain-derived neurotrophic
820 factor and the development of structural neuronal connectivity. Dev Neurobiol
821 70:271-288.
822 Conner JM, Lauterborn JC, Yan Q, Gall CM, Varon S (1997) Distribution of brain-
823 derived neurotrophic factor (BDNF) protein and mRNA in the normal adult rat
824 CNS: evidence for anterograde axonal transport. The Journal of neuroscience : the
825 official journal of the Society for Neuroscience 17:2295-2313.
826 Corson SL, Hill DL (2011) Chorda tympani nerve terminal field maturation and
827 maintenance is severely altered following changes to gustatory nerve input to the
828 nucleus of the solitary tract. J Neurosci 31:7591-7603.
829 Davies AM, Thoenen H, Barde YA (1986) The response of chick sensory neurons to
830 brain-derived neurotrophic factor. J Neurosci 6:1897-1904.
831 Davis BJ (1988) Computer-generated rotation analyses reveal a key three-dimensional
832 feature of the nucleus of the solitary tract. Brain Res Bull 20:545-548.
833 Farbman AI (1969) Fine structure of degenerating tast buds after denervation. J Embryol
834 Exp Morphol 22:55-68.
835 Fawcett JP, Bamji SX, Causing CG, Aloyz R, Ase AR, Reader TA, McLean JH, Miller
836 FD (1998) Functional Evidence that BDNF is an Anterograde Neuronal Trophic
837 Factor in the CNS. J Neurosci 18:2808-2821.
838 Frank ME (1991) Taste-responsive neurons of the glossopharyngeal nerve of the rat. J
839 Neurophysiol 65:1452-1463.
840 Ganchrow D, Ganchrow JR, Cicchini V, Bartel DL, Kaufman D, Girard D, Whitehead
841 MC (2014) Nucleus of the solitary tract in the C57BL/6J mouse: Subnuclear

842 parcellation, chorda tympani nerve projections, and brainstem connections. J
843 Comp Neurol 522:1565-1596.
844 Guagliardo NA, Hill DL (2007) Fungiform taste bud degeneration in C57BL/6J mice
845 following chorda-lingual nerve transection. J Comp Neurol 504:206-216.
846 Hellekant G, af Segerstad CH, Roberts T, van der Wel H, Brouwer JN, Glaser D, Haynes
847 R, Eichberg JW (1985) Effects of gymnemic acid on the chorda tympani proper
848 nerve responses to sweet, sour, salty and bitter taste stimuli in the chimpanzee.
849 Acta Physiol Scand 124:399-408.
850 Hill DL, Bradley RM, Mistretta CM (1983) Development of taste responses in rat
851 nucleus of solitary tract. J Neurophysiol 50:879-895.
852 Hoshino N, Vatterott P, Egwiekhor A, Rochlin MW (2010) Brain-derived neurotrophic
853 factor attracts geniculate ganglion neurites during embryonic targeting. Dev
854 Neurosci 32:184-196.
855 Hu B, Nikolakopoulou AM, Cohen-Cory S (2005) BDNF stabilizes synapses and
856 maintains the structural complexity of optic axons in vivo. Development
857 132:4285-4298.
858 Huang EJ, Reichardt LF (2001) Neurotrophins: roles in neuronal development and
859 function. Annu Rev Neurosci 24:677-736.
860 Huang T, Krimm RF (2010) Developmental expression of Bdnf, Ntf4/5, and TrkB in the
861 mouse peripheral taste system. Dev Dyn 239:2637-2646.
862 Je HS, Yang F, Ji Y, Nagappan G, Hempstead BL, Lu B (2012) Role of pro-brain-derived
863 neurotrophic factor (proBDNF) to mature BDNF conversion in activity-dependent

competition at developing neuromuscular synapses. Proc Natl Acad Sci U S A 109:15924-15929.

Kumari A, Ermilov AN, Grachtchouk M, Dlugosz AA, Allen BL, Bradley RM, Mistretta CM (2017) Recovery of taste organs and sensory function after severe loss from Hedgehog/Smoothened inhibition with cancer drug sonidegib. Proc Natl Acad Sci U S A 114:E10369-E10378.

Lasiter PS, Wong DM, Kachele DL (1989) Postnatal development of the rostral solitary nucleus in rat: dendritic morphology and mitochondrial enzyme activity. Brain Res Bull 22:313-321.

Levi-Montalcini R, Hamburger V (1951) Selective growth stimulating effects of mouse sarcoma on the sensory and sympathetic nervous system of the chick embryo. J Exp Zool 116:321-361.

Levi-Montalcini R, Cohen S (1956) In Vitro and in Vivo Effects of a Nerve Growth-Stimulating Agent Isolated from Snake Venom. Proc Natl Acad Sci U S A 42:695-699.

Levi-Montalcini R, Angeletti PU (1963) Essential role of the nerve growth factor in the survival and maintenance of dissociated sensory and sympathetic embryonic nerve cells in vitro. Dev Biol 7:653-659.

Lom B, Cohen-Cory S (1999) Brain-derived neurotrophic factor differentially regulates retinal ganglion cell dendritic and axonal arborization in vivo. J Neurosci 19:9928-9938.

885 Lom B, Cogen J, Sanchez AL, Vu T, Cohen-Cory S (2002) Local and target-derived
886 brain-derived neurotrophic factor exert opposing effects on the dendritic
887 arborization of retinal ganglion cells in vivo. J Neurosci 22:7639-7649.
888 Ma L, Lopez GF, Krimm RF (2009) Epithelial-derived brain-derived neurotrophic factor
889 is required for gustatory neuron targeting during a critical developmental period. J
890 Neurosci 29:3354-3364.
891 Mangold JE, Hill DL (2008) Postnatal reorganization of primary afferent terminal fields
892 in the rat gustatory brainstem is determined by prenatal dietary history. J Comp
893 Neurol 509:594-607.
894 May OL, Hill DL (2006) Gustatory terminal field organization and developmental
895 plasticity in the nucleus of the solitary tract revealed through triple-fluorescence
896 labeling. J Comp Neurol 497:658-669.
897 Mbiene JP, Mistretta CM (1997) Initial innervation of embryonic rat tongue and
898 developing taste papillae: nerves follow distinctive and spatially restricted
899 pathways. Acta Anat (Basel) 160:139-158.
900 Meng L, Ohman-Gault L, Ma L, Krimm RF (2015) Taste Bud-Derived BDNF Is
901 Required to Maintain Normal Amounts of Innervation to Adult Taste Buds.
902 eNeuro 2.
903 Nosrat CA, Ebendal T, Olson L (1996) Differential expression of brain-derived
904 neurotrophic factor and neurotrophin 3 mRNA in lingual papillae and taste buds
905 indicates roles in gustatory and somatosensory innervation. J Comp Neurol
906 376:587-602.

907 Nosrat CA, MacCallum DK, Mistretta CM (2001) Distinctive spatiotemporal expression
908 patterns for neurotrophins develop in gustatory papillae and lingual tissues in
909 embryonic tongue organ cultures. Cell Tissue Res 303:35-45.
910 Poo M (2001) Neurotrophins as synaptic modulators. Nat Rev Neurosci 2.
911 Ridler TW, Calvard S (1978) Picture Thresholding Using an Iterative Selection Method.
912 Ieee T Syst Man Cyb 8:630-632.
913 Ruzankina Y, Pinzon-Guzman C, Asare A, Ong T, Pontano L, Cotsarelis G, Zediak VP,
914 Velez M, Bhandoola A, Brown EJ (2007) Deletion of the developmentally
915 essential gene ATR in adult mice leads to age-related phenotypes and stem cell
916 loss. Cell Stem Cell 1:113-126.
917 Shingai T, Beidler LM (1985) Response characteristics of three taste nerves in mice.
918 Brain Res 335:245-249.
919 Singh KK, Miller FD (2005) Activity regulates positive and negative neurotrophin-
920 derived signals to determine axon competition. Neuron 45:837-845.
921 Singh KK, Park KJ, Hong EJ, Kramer BM, Greenberg ME, Kaplan DR, Miller FD (2008)
922 Developmental axon pruning mediated by BDNF-p75NTR-dependent axon
923 degeneration. Nat Neurosci 11:649-658.
924 Skyberg R, Sun C, Hill DL (2017) Maintenance of Mouse Gustatory Terminal Field
925 Organization Is Disrupted following Selective Removal of Peripheral Sodium Salt
926 Taste Activity at Adulthood. J Neurosci 37:7619-7630.
927 Sun C, Dayal A, Hill DL (2015) Expanded terminal fields of gustatory nerves accompany
928 embryonic BDNF overexpression in mouse oral epithelia. J Neurosci 35:409-421.

929 Sun C, Hummler E, Hill DL (2017) Selective Deletion of Sodium Salt Taste during
930 Development Leads to Expanded Terminal Fields of Gustatory Nerves in the
931 Adult Mouse Nucleus of the Solitary Tract. J Neurosci 37:660-672.
932 Thanos S, Bahr M, Barde YA, Vanselow J (1989) Survival and Axonal Elongation of
933 Adult Rat Retinal Ganglion Cells. Eur J Neurosci 1:19-26.
934 Thoenen H (1995) Neurotrophins and neuronal plasticity. Science 270:593-598.
935 Tonra JR (1999) Classical and novel directions in neurotrophin transport and research:
936 anterograde transport of brain-derived neurotrophic factor by sensory neurons.
937 Microsc Res Tech 45:225-232.
938 Tonra JR, Curtis R, Wong V, Cliffer KD, Park JS, Timmes A, Nguyen T, Lindsay RM,
939 Acheson A, DiStefano PS (1998) Axotomy upregulates the anterograde transport
940 and expression of brain-derived neurotrophic factor by sensory neurons. The
941 Journal of neuroscience : the official journal of the Society for Neuroscience
942 18:4374-4383.
943 Whitehead MC (1988) Neuronal architecture of the nucleus of the solitary tract in the
944 hamster. J Comp Neurol 276:547-572.
945 Whitehead MC, Frank ME, Hettinger TP, Hou LT, Nah HD (1987) Persistence of taste
946 buds in denervated fungiform papillae. Brain Res 405:192-195.
947 Yee CL, Jones KR, Finger TE (2003) Brain-derived neurotrophic factor is present in
948 adult mouse taste cells with synapses. J Comp Neurol 459:15-24.
949 Zheng S, Sun C, Hill D (2014) Postnatal reorganization of primary gustatory afferent
950 terminal fields in the mouse brainstem is altered by prenatal dietary sodium
951 history. ABSTRACT Society for Neurosciences.

952 Zhou XF, Rush RA (1996) Endogenous brain-derived neurotrophic factor is
953 anterogradely transported in primary sensory neurons. Neuroscience 74:945-953.
954
955

956 **LEGENDS**

957 **Figure 1.** Mean (±SEM) normalized expression levels of *Bdnf* in **(A)** the anterior tongue,
958 **(B)** geniculate ganglion, and **(C)** nucleus of the solitary tract (NST) in Control (black
959 bars), K14-*Bdnf* iKO No TAM (blue bars), and K14-*Bdnf* iKO (magenta bars) mice, and
960 mean (±SEM) normalized expression levels of *Bdnf* in **(D)** the anterior tongue, **(E)**
961 geniculate ganglion, and **(F)** nucleus of the solitary tract (NST) in Control (black bars),
962 UBC-*Bdnf* iKO No TAM (blue bars), and UBC-*Bdnf* iKO (magenta bars) mice. Means
963 were calculated relative to the respective expression levels in Control mice. The
964 expression ratio of 1.0 represents the Control mean. **G.** Photomicrograph of a horizontal
965 section through the anterior portion of the NST showing immunohistochemical labeling
966 to anti-BDNF in a Control (left) and a UBC-*Bdnf* iKO (right) mice. Asterisks in A-F
967 denotes significantly less than the respective No TAM group ($p < 0.05$). Scale bar in G =
968 100 µm. R-Rostral, L-Lateral. White lines in G denote outlines of NST.

969 **Figure 2. (A)** Mean (±SEM) total terminal field volumes for the IX, CT, and GSP nerves
970 and their double and triple overlaps of terminal fields in Control (black bars), *Bdnf* iKO
971 No TAM (blue bars), K14-*Bdnf* iKO (teal bars), and UBC-*Bdnf* iKO (magenta bars)
972 mice. Mean (±SEM) terminal field volumes for the IX, CT, and GSP nerves and their
973 double and triple overlaps of terminal fields in the **(B)** Far Dorsal Zone, **(C)** Dorsal Zone,
974 **(D)** Intermediate Zone, and **(E)** Ventral Zone of the NST in the same animals shown in
975 **A**.

976 # - significantly different than all other three groups.

977 * - significantly different than Control and *Bdnf* iKO No TAM mice.

978 **Figure 3. (A)** Horizontal sections of labeled terminal fields of IX (green), GSP (red), CT
979 (blue), and merged images of all three nerves (TRIPLE) for a *Bdnf* iKO No TAM (top
980 row for each Zone), a K14-*Bdnf* iKO (middle row of each panel), and a UBC-*Bdnf* iKO
981 mouse (bottom row of each panel). For the triple label photomicrographs, the CT-GSP
982 overlap is shown as magenta, the IX-GSP overlap is shown as yellow, the IX-CT overlap
983 in shown as blue-green, and the CT-GSP-IX terminal field overlap is shown as white
984 (Refer to the color guide in the panel for CT label in the Ventral Zone of the UBC-*Bdnf*
985 iKO mouse). Scale bar = 200µm. R, rostral; L, lateral. **(B)** Heat maps showing the
986 terminal field densities (volume of terminal field label in a division/total volume of the
987 division) for IX, CT, and GSP nerves, and for the triple overlap of all three nerve
988 terminal fields (TRIPLE) for *Bdnf* iKO No TAM mice (top row for each Zone), K14-
989 *Bdnf* iKO (middle row of each panel), and UBC-*Bdnf* iKO mice (bottom row of each
990 panel). The NST (borders shown in white) has been rotated so that the solitary tract is
991 oriented vertically (see Methods section and see R, rostral, and L, lateral orientations in
992 B, TRIPLE overlap). The NST for each zone is divided into a maximum of 100 X 100
993 pixel divisions for each optical image (see Methods). The colors for the heat map of
994 densities are on the relative scale shown for the Far Dorsal Zone in B, with 0% of
995 maximum density noted as dark blue and 100% noted as red. This relative scale was
996 applied to each of the four zones; therefore, the maximum density was obtained from all
997 of the divisions from *Bdnf* iKO No TAM, K14-*Bdnf* iKO, and UBC-*Bdnf* iKO mice for
998 the Far Dorsal Zone, and similarly for the Dorsal, Intermediate and Ventral Zones. The
999 division representing 100% (brightest red) for each zone is shown by a white border

1000 around the respective 100 X 100-pixel division (e.g., contained in the IX terminal field of
1001 UBC-*Bdnf* iKO mice in the Far Dorsal Zone).

1002 **Figure 4. A-J** Coronal sections through the rostral/ventral NST showing the IX nerve
1003 terminal field (green; A,B), GSP nerve terminal field labeling (red; C,D), CT nerve
1004 terminal field labeling (blue; E,F), and merged (G,H) terminal fields, and the terminal
1005 fields in the right hemifield of medulla captured with transmitted light (I,J) in a *Bdnf* iKO
1006 No TAM (A,C,E,F,I) and UBC-*Bdnf* iKO (B,D,F,H,J) mouse. The orientation of the
1007 sections is shown in E. D, Dorsal; L, Lateral. The color wheel for the merged images is
1008 shown in G. Scale bars: H, 200 μm; J, 500 μm. The white lines shown in I and J
1009 demarcate the NST. 4V, Fourth ventricle; 7, Facial nucleus; DC, Dorsal cochlear nucleus;
1010 icp, inferior cerebellar peduncle; MVePC, Medial vestibular nucleus, parvicellular; sol,
1011 solitary tract; Sp5O, spinal trigeminal nucleus, oral; SpVe, spinal vestibular nucleus.

1012 **Figure 5. (A)** Integrated taste responses from the chorda tympani nerve (CT) in a Control
1013 (top panel), K14-*Bdnf* iKO (middle panel), and a UBC-*Bdnf* iKO mouse to a
1014 concentration series of NaCl and to 0.5M NH_4Cl. Scale bar shown near response to 0.5M
1015 NH_4Cl in UBC-*Bdnf* iKO mouse = 20 sec. **B.** Mean (± SEM) relative taste responses to a
1016 concentration series of NaCl from the CT in Control, K14-*Bdnf* iKO No TAM, and K14-
1017 *Bdnf* iKO mice before (solid lines) and with lingual application of amiloride (dotted
1018 lines). **C.** Mean (± SEM) relative taste responses to a concentration series of NaCl from
1019 the CT in control, UBC-*Bdnf* iKO No TAM, and UBC-*Bdnf* iKO mice before (solid lines)
1020 and with lingual application of amiloride (dotted lines).

1021 **Table 1.** Table showing the specific measure tested (MEASURE), the factor (FACTOR),
1022 degrees of freedom (df), F value (F), and significance (SIGNIFICANCE) of each

1023 Analysis of Variance (ANOVA) statistical tests presented in the Results section. They
1024 appear in the order presented in the Results section.
1025
1026 **Table 2.** Table showing the Mean, SEM, and number of animals/group (n) for relative
1027 taste responses from the CT to a concentration series of NaCl before and after lingual
1028 application to amiloride, and to a concentration series of citric acid, sucrose, and quinine
1029 hydrochloride in Controls, K14-*Bdnf* iKO No TAM, and K14-*Bdnf* iKO mice and for the
1030 CT in Controls, UBC-*Bdnf* iKO No TAM, and UBC-*Bdnf* iKO mice.

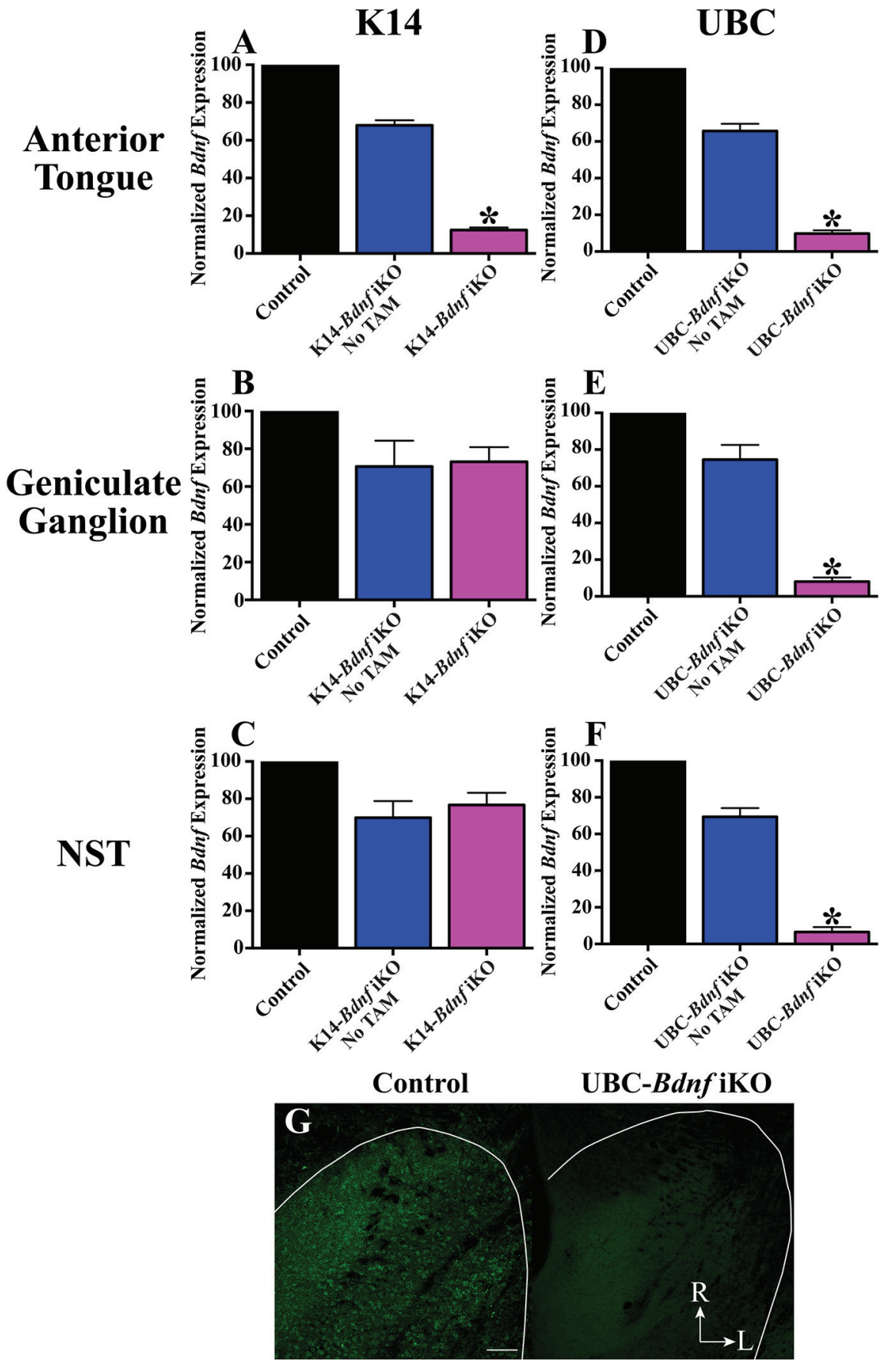

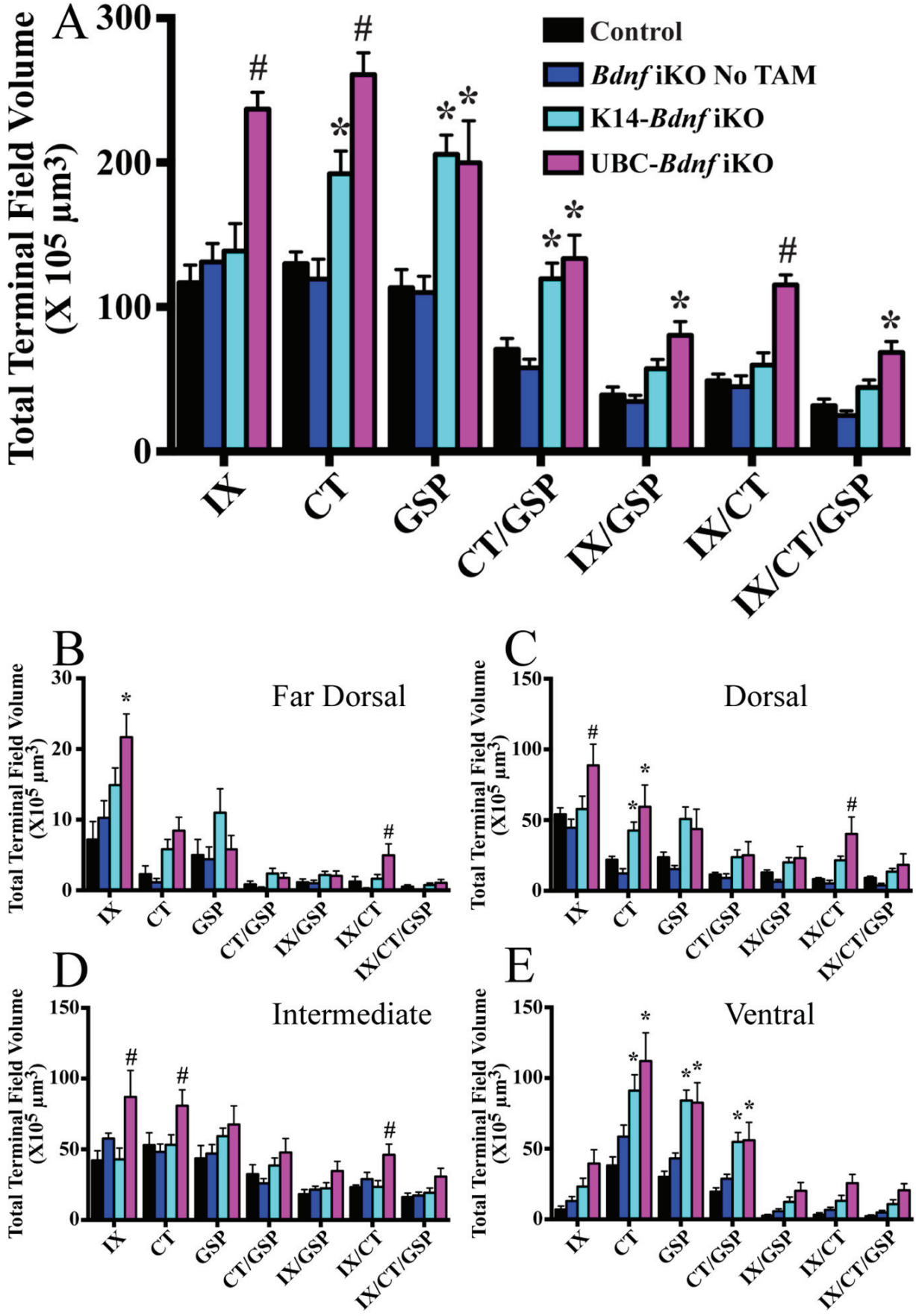

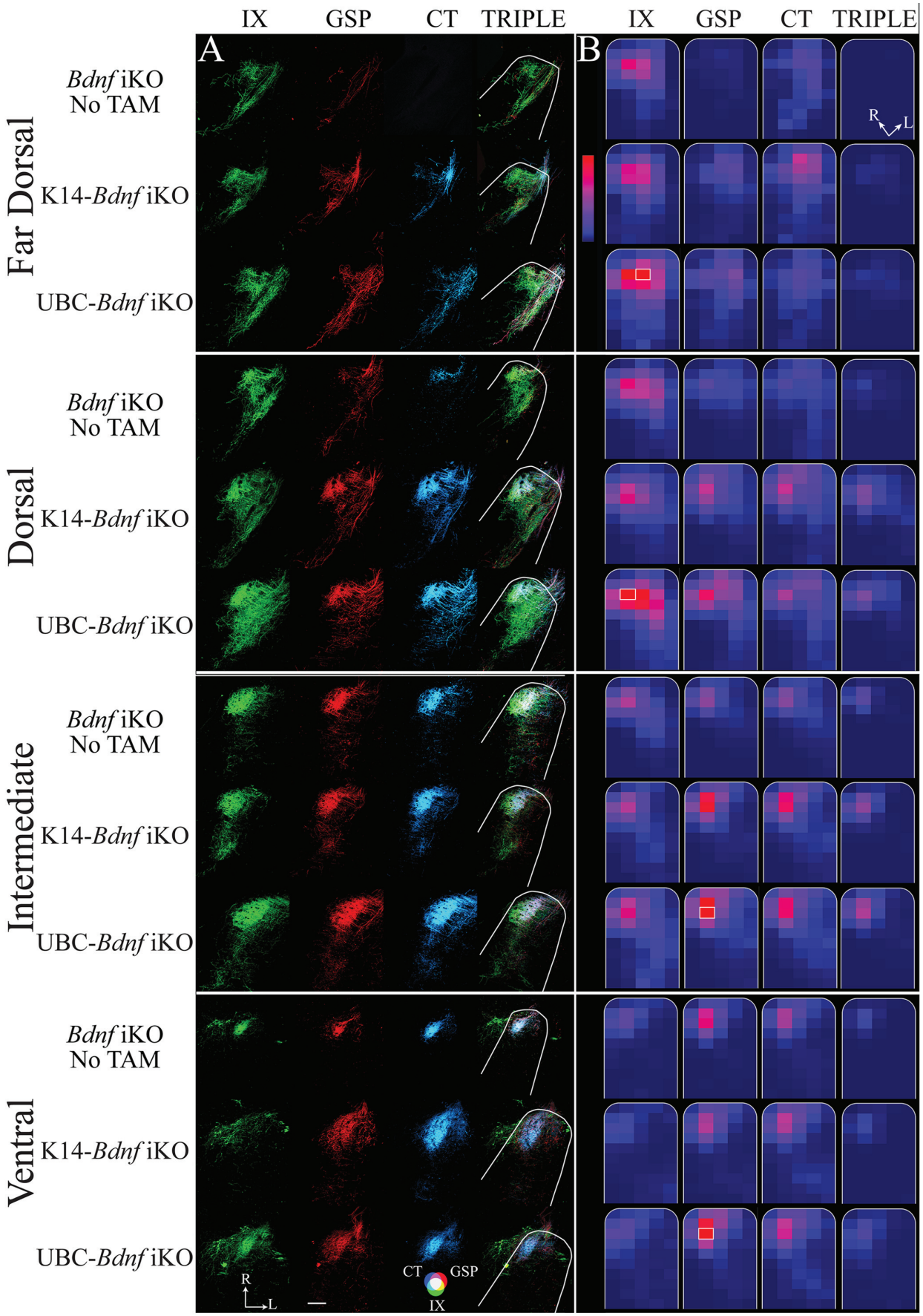

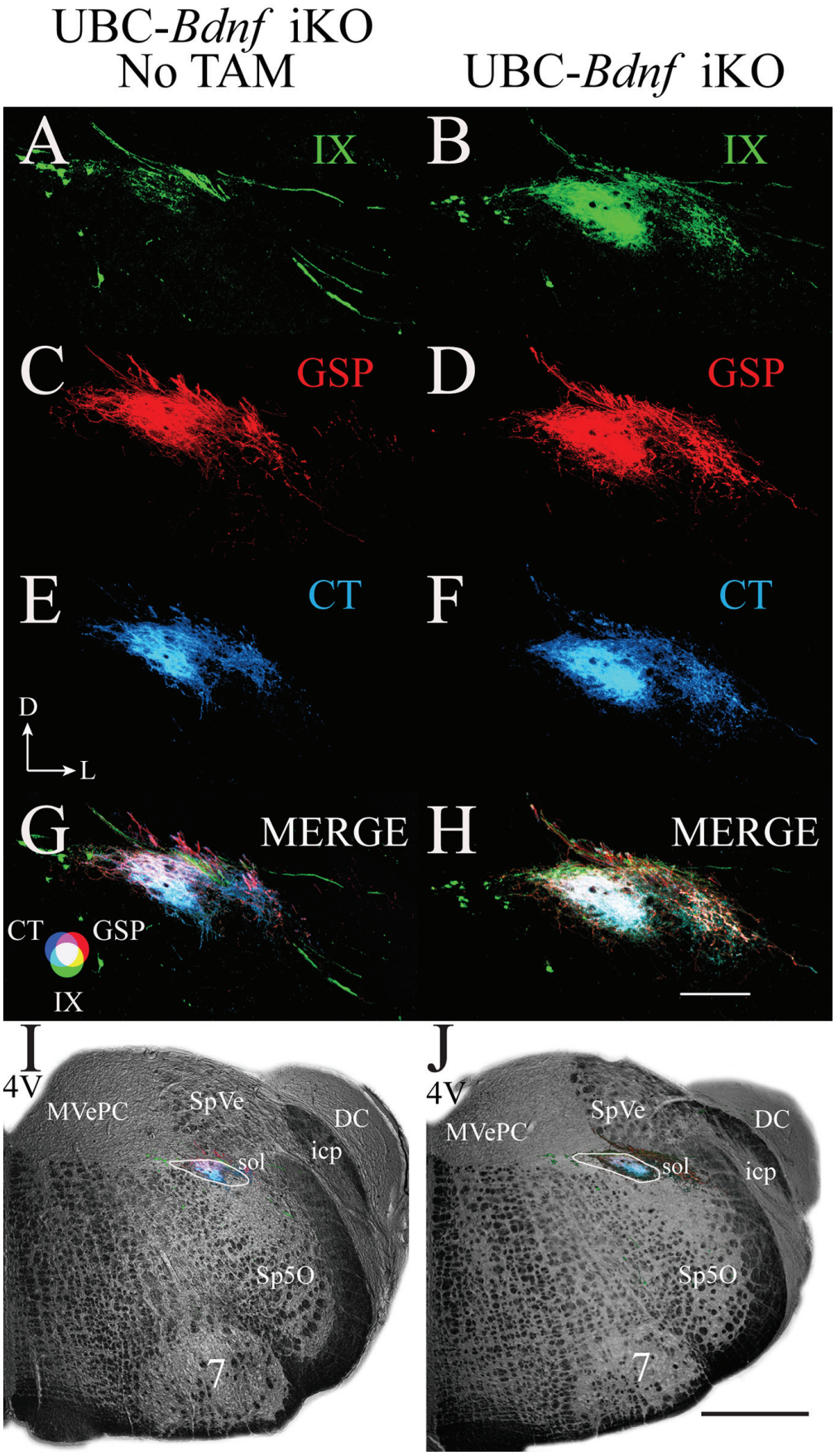

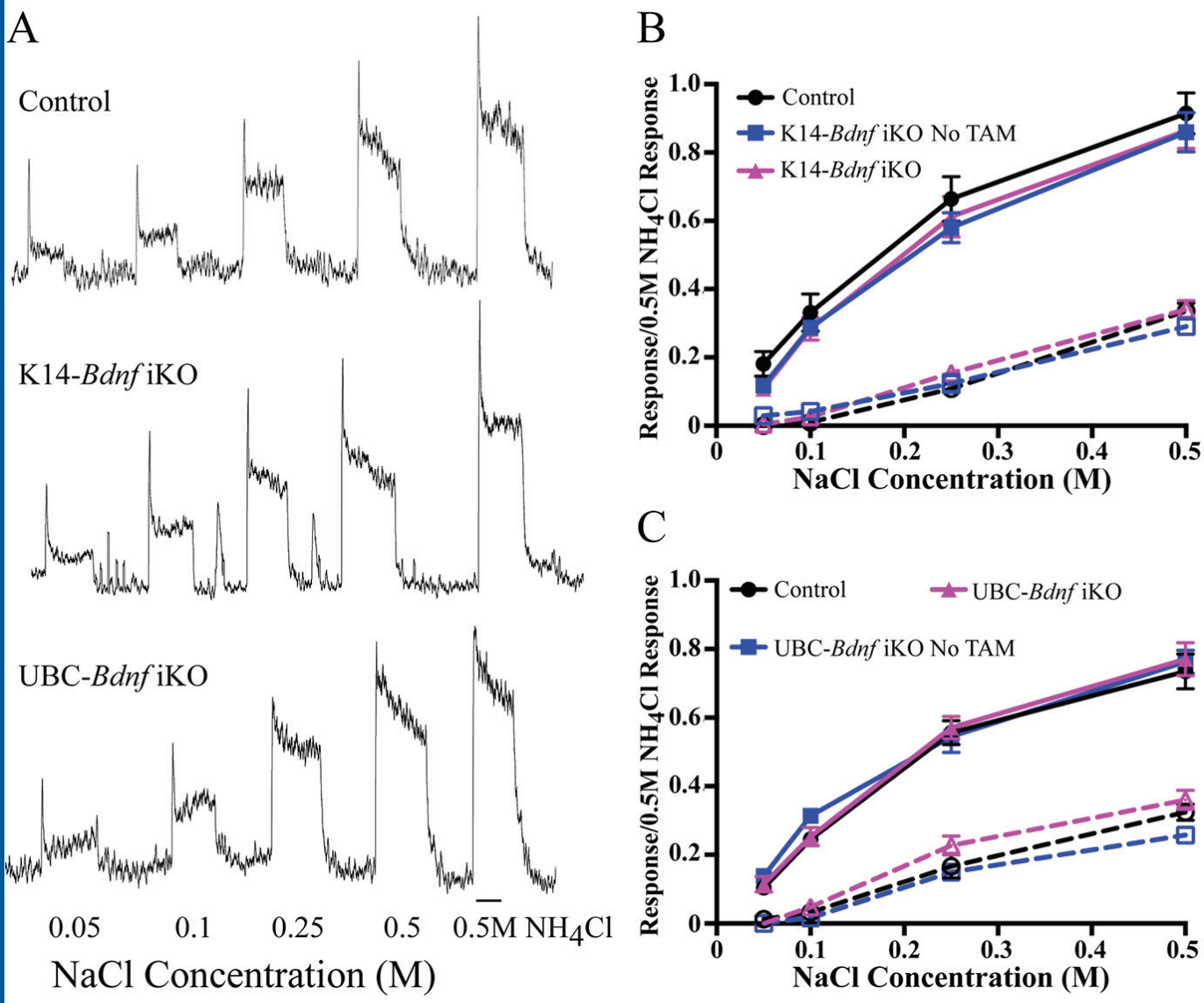

TABLE 1 -- ANOVA Results

MEASURE	FACTOR	df	F	SIGNIFICANCE
Total Volume--Single Nerves	Group	3,63	35.1	0.0001
Total Volume--Single Nerves	Group X Nerve	6,63	2.9	0.02
Total Volume--Overlap	Group	3,84	45.3	0.0001
Total Volume--Overlap	Group X Nerve	9,84	2.5	0.02
Far Dorsal Volume--Single Nerves	Group	3,63	7.7	0.0001
Far Dorsal Volume--Single Nerves	Group X Nerve	6,63	1.7	0.12
Far Dorsal Volume--Overlap	Group	3,84	9.8	0.0001
Far Dorsal Volume--Overlap	Group X Nerve	9,84	2.2	0.03
Dorsal Volume--Single Nerves	Group	3,63	14.2	0.0001
Dorsal Volume--Single Nerves	Group X Nerve	6,63	1.1	0.39
Dorsal Volume--Overlap	Group	3,84	16.2	0.0001
Dorsal Volume--Overlap	Group X Nerve	9,84	1.1	0.39
Intermediate Volume--Single Nerves	Group	3,63	6.8	0.0001
Intermediate Volume--Single Nerves	Group X Nerve	6,63	1.2	0.34
Intermediate Volume--Overlap	Group	3,84	9.9	0.0001
Intermediate Volume--Overlap	Group X Nerve	9,84	0.6	0.76
Ventral Volume--Single Nerves	Group	3,63	22.9	0.0001
Ventral Volume--Single Nerves	Group X Nerve	6,63	1.7	0.13
Ventral Volume--Overlap	Group	3,84	22.8	0.0001
Ventral Volume--Overlap	Group X Nerve	9,84	1.9	0.06
Ganglion Count	Group	2,40	0.7	0.52
Ganglion Count	Nerve	2,40	99.9	0.0001
Ganglion Count	Group X Nerve	4,40	0.3	0.89

K14-*Bdnf* iKO mice				
NaCl Taste Response	Group	2,16	0.8	0.47
NaCl Taste Response	Group X Concentration	6,48	0.1	0.99
NaCl After Amiloride	Group	2,14	0.5	0.65
NaCl After Amiloride	Group X Concentration	6,42	2.8	0.02
Citric Acid Taste Response	Group	2,18	1.2	0.31
Citric Acid Taste Response	Group X Concentration	4,36	2.7	0.05
Sucrose Taste Response	Group	2,19	0.2	0.83
Sucrose Taste Response	Group X Concentration	6,57	0.9	0.47
Quinine Taste Response	Group	2,18	0.6	0.55
Quinine Taste Response	Group X Concentration	6,54	0.6	0.72
UBC-*Bdnf* iKO mice				
NaCl Taste Response	Group	2,18	0.4	0.69
NaCl Taste Response	Group X Concentration	6,54	0.6	0.75
NaCl After Amiloride	Group	2,16	3.5	0.06
NaCl After Amiloride	Group X Concentration	6,48	1.6	0.18
Citric Acid Taste Response	Group	2,21	0.6	0.54
Citric Acid Taste Response	Group X Concentration	4,42	1.9	0.12
Sucrose Taste Response	Group	2,17	0.1	0.92
Sucrose Taste Response	Group X Concentration	6,51	0.6	0.72
Quinine Taste Response	Group	2,19	0.0	0.99
Quinine Taste Response	Group X Concentration	6,57	0.6	0.70

TABLE 2 – Mean (± SEM) Taste Responses
(Response/0.5M NH_4Cl Response)

NaCl

	Controls			K14-*Bdnf* iKO No TAM			K14-*Bdnf* iKO		
Concentration (M)	Mean	± SEM	N	Mean	± SEM	N	Mean	± SEM	N
0.05	0.181	0.04	8	0.117	0.02	6	0.108	0.01	5
0.10	0.331	0.05	8	0.287	0.02	6	0.284	0.03	5
0.25	0.664	0.07	8	0.580	0.04	6	0.612	0.06	5
0.50	0.915	0.06	8	0.859	0.06	6	0.864	0.05	5

NaCl with amiloride

	Controls			K14-*Bdnf* iKO No TAM			K14-*Bdnf* iKO		
Concentration (M)	Mean	± SEM	N	Mean	± SEM	N	Mean	± SEM	N
0.05	0.000	0.00	6	0.030	0.02	6	0.004	0.00	5
0.10	0.010	0.01	6	0.042	0.02	6	0.026	0.01	5
0.25	0.108	0.02	6	0.124	0.03	6	0.154	0.02	5
0.50	0.336	0.02	6	0.290	0.01	6	0.340	0.03	5

NaCl

	Controls			UBC-*Bdnf* iKO No TAM			UBC-*Bdnf* iKO		
Concentration (M)	Mean	± SEM	N	Mean	± SEM	N	Mean	± SEM	N
0.05	0.104	0.02	8	0.138	0.02	6	0.115	0.02	7
0.10	0.245	0.02	8	0.314	0.02	6	0.253	0.03	7
0.25	0.556	0.04	8	0.545	0.05	6	0.571	0.03	7
0.50	0.735	0.05	8	0.763	0.03	6	0.770	0.05	7

NaCl with amiloride

	Controls			UBC-*Bdnf* iKO No TAM			UBC-*Bdnf* iKO		
Concentration (M)	Mean	± SEM	N	Mean	± SEM	N	Mean	± SEM	N
0.05	0.013	0.01	7	0.000	0.00	5	0.006	0.00	7
0.10	0.032	0.02	7	0.016	0.01	5	0.049	0.02	7
0.25	0.167	0.03	7	0.150	0.01	5	0.227	0.03	7
0.50	0.324	0.02	7	0.258	0.02	5	0.360	0.03	7

Citric Acid

	Controls			K14-*Bdnf* iKO No TAM			K14-*Bdnf* iKO		
Concentration (mM)	Mean	± SEM	N	Mean	± SEM	N	Mean	± SEM	N

10	0.126	0.04	9	0.185	0.07	6	0.191	0.04	9
20	0.320	0.04	9	0.356	0.06	6	0.476	0.04	9
50	0.588	0.04	9	0.511	0.07	6	0.642	0.06	9

Citric Acid

	Controls			UBC-*Bdnf* iKO No TAM			UBC-*Bdnf* iKO		
Concentration (mM)	Mean	± SEM	N	Mean	± SEM	N	Mean	± SEM	N
10	0.143	0.05	7	0.154	0.05	6	0.165	0.02	9
20	0.356	0.04	7	0.330	0.06	6	0.376	0.04	9
50	0.620	0.05	7	0.583	0.06	6	0.627	0.06	9

Sucrose

	Controls			K14-*Bdnf* iKO No TAM			K14-*Bdnf* iKO		
Concentration (M)	Mean	± SEM	N	Mean	± SEM	N	Mean	± SEM	N
0.10	0.237	0.06	9	0.241	0.09	6	0.323	0.07	7
0.25	0.462	0.08	9	0.508	0.12	6	0.536	0.08	7
0.50	0.529	0.07	9	0.604	0.09	6	0.571	0.08	7
1.00	0.544	0.06	9	0.605	0.08	6	0.566	0.07	7

Sucrose

	Controls			UBC-*Bdnf* iKO No TAM			UBC-*Bdnf* iKO		
Concentration (M)	Mean	± SEM	N	Mean	± SEM	N	Mean	± SEM	N
0.10	0.237	0.06	9	0.196	0.04	5	0.253	0.04	6
0.25	0.462	0.08	9	0.382	0.04	5	0.492	0.09	6
0.50	0.529	0.07	9	0.519	0.08	5	0.548	0.08	6
1.00	0.544	0.06	9	0.565	0.09	5	0.524	0.06	6

Quinine HCl

	Controls			K14-*Bdnf* iKO No TAM			K14-*Bdnf* iKO		
Concentration (mM)	Mean	± SEM	N	Mean	± SEM	N	Mean	± SEM	N
10	0.060	0.02	9	0.084	0.02	6	0.104	0.02	6
20	0.121	0.05	9	0.147	0.02	6	0.154	0.04	6
50	0.265	0.04	9	0.275	0.06	6	0.315	0.05	6
100	0.282	0.03	9	0.381	0.06	6	0.328	0.04	6

Quinine HCl

	Controls			UBC-*Bdnf* iKO No TAM			UBC-*Bdnf* iKO		
Concentration (mM)	Mean	± SEM	N	Mean	± SEM	N	Mean	± SEM	N

10	0.060	0.02	9	0.030	0.03	7	0.063	0.05	6
20	0.121	0.05	9	0.089	0.03	7	0.097	0.04	6
50	0.265	0.04	9	0.294	0.04	7	0.265	0.06	6
100	0.282	0.03	9	0.311	0.04	7	0.310	0.05	6